THE RHEOLOGY OF ASPHALT

by

RICHARD RAMSAY STANDER, JR.
BSCE, The Ohio State University
(1965)

Submitted in partial fulfillment
of the requirements for the degree of
Master of Science

at the
Massachusetts Institute of Technology

(1966)

Signature of Author . . . . . .
Department of Civil Engineering, May 20, 1966

Certified by . . . . . .
Thesis Supervisor

Accepted by . . . . . .
Chairman, Departmental Committee on Graduate Students

ABSTRACT

THE RHEOLOGY OF ASPHALT

by

RICHARD RAMSAY STANDER, JR.

Submitted to the Department of Civil Engineering on May 20, 1966, in partial fulfillment of the requirements for the degree of Master of Science.

This study briefly reviews some concepts suggested to analyze the flow characteristics of rheological materials with emphasis on those which are promising in the analysis of flow of asphalts. The suggested concepts are catagorized as experimental, mathematical, structural, physical-chemical, and thermal. It is shown that for the three asphalts used, it is possible to construct flow diagrams over a wide range of shear stress, shear rate, and temperature using different viscometers and the principle of reduced variables. Thermodynamic analysis is used to study thermal characteristics of flow behavior. An application of Eyring's rate process theory to the analysis of asphalt flow is examined and the variation of viscosity, determined at constant shear stress or constant shear rate, with temperature is discussed.

Thesis Supervisor: Dr. F. Moavenzadeh

Title: Associate Professor of Civil Engineering

ACKNOWLEDGEMENT

To Dr. Fred Moavenzadeh, whose time given to this author not only culminated his educational experience, but inspired this thesis. He will always have the author's sincerest respect and gratitude.

Appreciation is also extended to A. Shima, A. Rao, P. Rad, and the many other staff members of the materials lab of Ohio State University, Department of Civil Engineering, who were of great assistance in researching the test data for this thesis.

To the Ohio Department of Highways and the Bureau of Public Roads which provided the funds for this research, thank you.

Special thanks to Mrs. Joan Handelsman whose professional digital manipulations gave these ideas form.

A special debt of gratitude to my wife, whose patience and understanding made the writing of this thesis possible.

TABLE OF CONTENTS

LIST OF TABLES AND FIGURES

INTRODUCTION

The trend of research on the rheological properties of asphaltic materials has been in the direction of stress-strain viscosity characteristics over wide ranges of temperature. However, the complex chemical structure and numerous varieties of asphalt have thus far, prevented the development of a specific mechanism for describing its flow behavior over the useful range of loading and climatic variables. There are, however, a great number of empirical models, relatively few semi-empirical models, and few theoretical models proposed to describe the flow behavior of asphaltic materials over a limited range of some specific variables. The extent of work in this area was well reviewed by Schweyer in 1958(1)*. "Acceptance of the statement that 'knowledge in a field is measured by the brevity with which the concepts can be presented' makes the asphalt technologist pause when the voluminous literature on asphalt is considered." This,

---

*Note: Numbers in parentheses refer to the List of References.

in other words, indicates that the "art of asphalt" is a very real and necessary part of asphalt technology, and, in order to achieve a scientific base for this "art," fundamental concepts involving the flow properties of asphalt must be developed.

It is, therefore, the purpose of this investigation to study the flow behavior of paving asphalts, and to apply flow data to various rheologic models with special interest in the hyperbolic sine model as developed by Eyring.

REVIEW OF LITERATURE

The objective of rheology is to yield a distinct fundamental, or rational, description of the deformation and flow of matter. To achieve this end the physical chemist has approached the problem by considering the molecular characteristics of materials. The mathematician has approached the problem by formulating the constitutive and/or conservative equations of the particular materials. Although advances in both fields are quite evident, the practical requirements of industry have outrun basic research. This situation has created analytical and empirical solutions based on simplifying assumptions as applied to observed flow conditions. More than ever, the applied approach has become that of using as much as possible of the physical-chemical and continuum mechanic works(2,3).

Flow Representation

In general, there are two basic methods used to represent the flow of a fluid; a shear stress-shear rate diagram or a viscosity-shear rate diagram.

The simplest plot of flow data is that of shear

stress versus shear rate on arithmetic coordinates. A Newtonian material will plot as a straight line passing through the origin. If the material is non-Newtonian, the data will, in general, pass through the origin but will not be linear. The disadvantage of this plot is that the degree of deviation from Newtonian characteristics cannot be determined, but, this can be accomplished in most cases by using a logrithmic plot. Generally, the data will describe a straight line which may be represented by a power formula:

$$\tau = A(\dot{\gamma})^n \qquad (1)$$

where τ is shear stress, $\dot{\gamma}$ is shear rate, A is the constant of proportionality, and n is a measure of the deviation from Newtonian behavior. For a Newtonian material, n is equal to unity.

Consistency cannot be represented by A because of dimensional difficulties; however, the viscosity, defined as $\tau/\dot{\gamma}$ for a given $\dot{\gamma}$ (sometimes referred to as apparent viscosity), may be used. Since the $\dot{\gamma}$ used is arbitrary, and in general not standardized, confusion may result. An alternate method is proposed by Traxler(4) in which viscosities are compared at a particular power input per volume of sample. Although

the power input is arbitrary ($\tau \times \dot{\gamma}$ =1,000 per unit volume given as convenient) the method has the advantage that very little extrapolation of data is necessary to determine values over wide ranges of materials and test temperatures. The degree of data treatment required to arrive at the basic shear diagram generally depends on the geometry of the test apparatus used.

An alternate method of representation of the rheologic response of materials is in terms of viscosity. For Newtonian materials, viscosity is defined as the ratio of shear stress to shear rate, which at constant temperature is in-dependent of the level of shear stress and/or shear rate. For non-Newtonian materials the ratio of shear stress to the corresponding shear rate is defined as the apparent viscosity and is shear dependent. For such materials, the slope of the shear diagram , $\partial\tau/\partial\dot{\gamma}$ is also used as a measure of viscosity and is referred to as the differential viscosity, η_D . Besides the apparent viscosity and the differential viscosity, a third term referred to as the plastic viscosity (η_P) is also used. This is defined as the slope of the straight line portion of the plot of $\dot{\gamma}$ versus τ

on arithmetic scales. Such a viscosity is independent of shear rate and is generally used to determine the yield stress of pseudoplastic materials.

Non-Newtonian flow behavior is usually referred to as either shear thinning or shear thickening. The first term would apply to the ideal Bingham plastics and the pseudoplastics. They both exhibit decreasing apparent viscosity with increasing shear rate. The term thixotropy, as sometimes applied to this whole group, is used here to describe a special case of shear thinning that is time dependent. The structure, which is broken down by shearing, is recoverable with time, or, in other words, the process is reversable. Dilatancy is sometimes used to describe shear thickening materials, however, this is a misnomer in that many materials which show increasing viscosity with increasing shear do not dilate at all. Thus, dilatancy is a special case of shear thickening.

Another unfortunate misuse of terms results by describing time dependent, shear thickening behavior as rheopectic. There may exist a material which displays shear thickening with time, but rheopexy is the process by which certain thixotropic materials regain their structure faster with the application of a gentle

shear. This is analogous to the flocculation process which is speeded up by a gentle stirring action. In both cases, increasing the shear beyond a certain limit will start to destroy the structure.

Experimental Interpretation

The basic objective of data interpretation is the prediction of flow properties given limited information. Until the development of a fundamental concept describing the flow behavior of materials in general, use of the existing models is generally limited to the range of variables incorporated in the development of such models. Thus application of these models, while showing good results when properly employed, is limited to the exact test conditions and materials as those used in the development of the particular relationship. In other words, these equations are usually used to cover a very specific range of data.

Each experimental relationship has, and will continue to serve its purpose, but the limitations and conditions of each must be thoroughly known before it can be applied meaningfully.

Mathematical Interpretation

To examine the flow behavior from the standpoint of continuum mechanics, certain relationships regarding the state of the material must be derived. These equations, commonly called the equations of change, are the relationships for conservation of mass, momentum, and mechanical and thermal energy.

By using these equations, singularly or in combination, flow problems may be set up, and with the help of numerous assumptions, the resulting relationships may be reduced to a solvable state. The difficulty in applying the equations of change to practical flow problems is that in all but a few select cases, the simplifying assumptions that are necessary damage the validity of the analysis so that the results are of questionable value. Currently, however, researchers in this area are applying as much as possible of the mathematical approach to empirically developed models.

Structural Interpretation

In recent years, the most promising approach toward developing a general theory of flow has been the structural interpretation. Four basic procedures have

been suggested depending on whether colloidal, elastic, kinetic, or rate theory is used as the basis of the argument. Of the four, colloidal theory is the oldest and simplest, and is based on low concentrations of particles in a solvent.

Using the basic idea that relative viscosity -- the solution viscosity divided by the solvent viscosity -- is a function of the energy dissipation caused by the presence of the suspended particles, relationships have been developed for particles of varied shapes at a range of concentrations. The effects of particle interaction, absorption of the solvent, particle deformability, system thermodynamic conditions, and system electral conditions have also been investigated in the light of colloidal theory(5).

The second concept of structural flow involves the suggestion first made by Maxwell(6), that liquids are elastic bodies with very high rates of stress relaxation. Basically, the hypothesis, as developed by Mooney(7), may be described as external applied forces causing a local stress and expansion within the material. When the expansion reaches a critical point, the local structure loses its rigidity and a molecular rearrangement takes place. This action in turn reduces the local stresses

to zero and reestablishes the normal rigidity. Mooney found that agreement could be established with published data provided adjustments that were expected or understandable were made on the values of the adjustable parameters.

The third concept of structural flow is based on a homogeneous reaction kinetic approach as developed by Denny and Brodkey (8,9). The basic hypothesis is that non-Newtonian materials show non-linear behavior because of a breakdown of the forces between particles. At very low shear rates there is no breakdown and the viscosity is a constant, η_o . At high shear rates all of the forces are broken, and again viscosity is constant, η_∞ . At any point between these extremes the tangential viscosity, η , is some function of the portion of the unbroken forces.

Majidzadeh and Schweyer(3), working with thirteen different asphalts, applied kinetic reaction theory to their data to determine an equilibrium constant, K, as a function of shear rate. If the equilibrium constant of a material and its limiting viscosities are known, the viscosity for any shear rate within the range of the study may be calculated knowing one additional point. The only requirements on the material are that it may

be represented by a hyperbolic sine relationship. The attractions of this theory are that the exact nature of the fundamental flow mechanism is not assumed, and that the constants are easy to determine and interpret.

The last approach is that of Eyring and his co-workers. As stated by Brodkey, "Their work is based on the application of theory of rate processes to the relaxation processes that are believed to play an important part in determining the nature of the flow. --- Very briefly, the theory postulates an activated complex as an intermediate unstable state, which would be formed from the reactants and decompose into the products. The assumption is made that the decomposition of the complex is the rate controlling step, and that there is an activation energy associated with this (10)." To expand this argument, the following is presented as digested from Glasstone et al. (11).

Liquids and gases may be considered as opposites, one consisting of matter moving around holes (gases), and the other, holes moving around matter. The energy necessary to provide molecular movement in a liquid is made up of two parts, the energy to create a hole, and the energy to move a molecule into it.

Consider, as in figure 1, a molecule occupying a volume $\delta_1 \delta_2 \delta_3$ where δ_1, δ_2, and δ_3 are center to center distances along the three axes. If δ is the distance between positions of equilibrium, then to move this distance the molecule must be transported across an energy barrier of magnitude E_o at absolute zero as shown in figure 2. This E_o is the so-called energy of activation. If one dimensional movement in the transverse direction is assumed, and if either direction is equally likely, then by applying a shearing force, F, the balance of the system is upset by the amount $2[\frac{1}{2} F \delta \delta_2 \delta_3]$. Further, if k is the initial rate of motion, then the movement in the direction of F may be written $k \exp(\frac{1}{2} F \delta \delta_2 \delta_3)$ and similarly the opposite movement is $k \exp(-\frac{1}{2} F \delta \delta_2 \delta_3)$. For a layer of molecules to move a distance δ the net rate of flow is then $\delta k (e^{\frac{1}{2} F \delta \delta_2 \delta_3} - e^{-\frac{1}{2} F \delta \delta_2 \delta_3})$ which is $2 \delta k \sinh(F \delta \delta_2 \delta_3 / 2KT)$. Dividing by the distance between molecules normal to the direction of flow gives:

$$\gamma^o = \frac{2\delta}{\delta_1} k \sinh\left(F \delta \delta_2 \delta_3 / 2KT\right) \qquad (2)$$

The value of k as derived from statistical considerations is:

$$k = \frac{KT}{h} \exp\left(-\Delta F / RT\right) \qquad (3)$$

where K, h, and R are respectively Boltzmann's, Planck's,

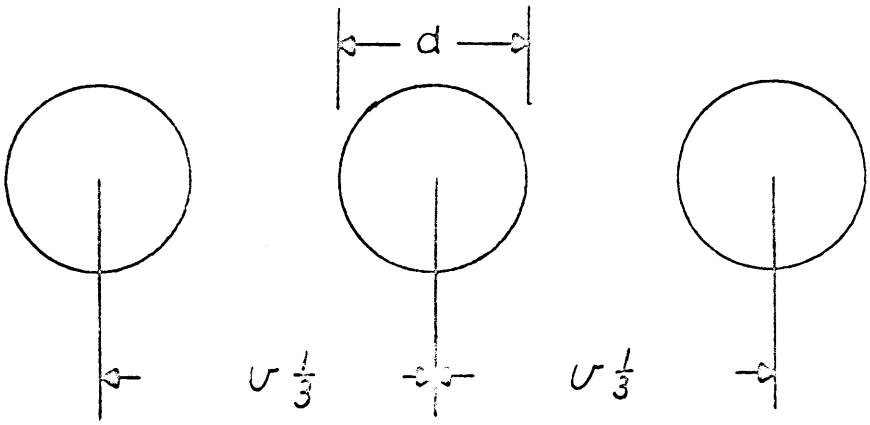

Figure 1 - Molecules Cut by a One-dimensional Plane.

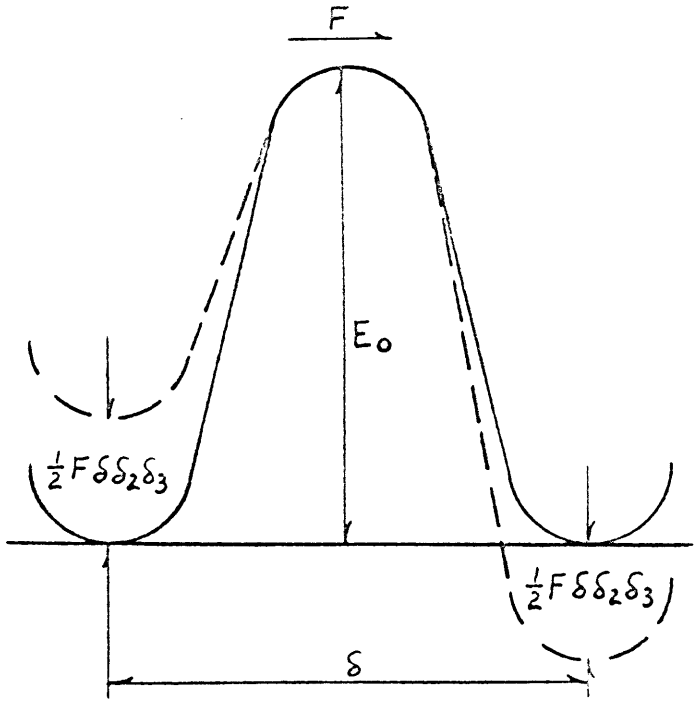

Figure 2 - The Energy Barrier, Theory of Rate Processes.

and the universal gas constants. This result applied to equation (2) gives the shear rate as:

$$\dot{\gamma} = 2\frac{\delta}{\delta_1}\frac{KT}{h}\exp(-\Delta F/RT)\sinh\left[\frac{F\delta\delta_2\delta_3}{2KT}\right] \qquad (4)$$

Herrin and Jones (2) applied this theory to asphalt assuming that $2\delta/\delta_1$ could be considered as approximately equal to unity. Using this assumption and the relation $\Delta F = \Delta H - T\Delta S$ where ΔF is the free energy of activation, ΔH is the heat of activation, and ΔS is the entropy of the system, they found that equation (4) could be reduced to:

$$\dot{\gamma} = \dot{\gamma}_o \sinh[\tau/\tau_o] \qquad (5)$$

where

$$\dot{\gamma}_o = \left(\frac{KT}{h}\right) e^{-\frac{\Delta H}{RT}} e^{\frac{\Delta S}{R}} \qquad (6)$$

and

$$\tau_o = 2KT/V_f \qquad (7)$$

Rewriting the expression for $\dot{\gamma}_o$ in logarithmic form:

$$\log \dot{\gamma}_o/T = \log K/h + \frac{\Delta S}{2.303R} - \frac{\Delta H}{2.303R}\left(\frac{1}{T}\right) \qquad (8)$$

Therefore, if $\dot{\gamma}_o$ is constant at any T, the plot of log $\dot{\gamma}_o/T$ versus $1/T$ would be a straight line. Data for the material used by Herrin and Jones validated this relationship.

It was shown that if τ_o is taken large compared to τ, then $\dot{\gamma} = \dot{\gamma}_o^{\circ} \tau / \tau_o$ and τ_o may be calculated at any test temperature from the semi-log plot $\dot{\gamma}_o^{\circ}/T$ versus $1/T$ for any selected $\dot{\gamma}^{\circ}$. Using this τ_o in equation (7), the flow unit size, V_f, at any temperature may be found. It was further shown that ΔS was not a function of temperature, and thus the heat of activation could be found as the slope of the plot. Since the intercept of the line is ΔS, the free energy of activation, ΔF, was found to be a linear function of temperature.

This analysis, applied to one asphalt showed that its flow behavior could be predicted using absolute rate theory. It also showed that the flow unit size was much larger than the individual molecules, and that they decreased in size as the temperature increased.

Physical-Chemical Interpretation

The earliest attempts to find a rational explanation for flow behavior in bitumens were based on physical-chemical systems. Nellensteyn (12) postulated a flow theory based on a colloidal system. His observations were of solutions of bitumens in benzene.

Mack (13) questions the validity of extrapolation of Nellensteyn's findings to a solvent-free material,

because evidence leads to the fact that asphaltenes are not completely dissolved in benzene, rather they exist in the solution as partially saturated associated particles. This is not compatable with the assumption that the asphaltic bitumens are solutions of asphaltenes in petrolenes which at low temperatures, less than 120° C., form molecular complexes. Mack shows qualitively that non-Newtonian flow increases as the aromaticity of the oil constituents decreases. Thus, it would seem that non-Newtonian flow is some function of the concentration of the asphaltenes, and the aromaticity or the ability of the petrolenes to dissolve the asphaltenes.

This work is substantiated by several studies on asphalt using the electron microscope. Katz and Betu (14) found that photographs of films of bitumens formed from benzene solutions showed associated particles of asphaltenes. Swanson (15), on the other hand, found that to form a homogeneous bitumen film by the same process, the ratio of resins to asphaltenes had to be at least three to one. Finally, if the film was not formed by evaporation of benzene from a bitumen-benzene solution, examination indicated no particles of typical colloidal dimensions.

To relate structure to flow properties, it is necessary to consider the shape of the associated com-

plexes. Considering the internal thermodynamics of the system, change will take place spontaneously only if the free energy is diminished. This decrease is associated with a decrease in surface area, and thus it could be expected that the complexes are spherical in shape. On application of a shear stress the particles elongate into ellipsoids and flow through the oily medium. In the case of Newtonian materials, the association bonds within the particles are too strong to be broken by the applied stress. On application of higher stresses, some point is reached where these bonds begin to break, and continue to break until breakup is in equilibrium with the applied stress. The material then shows Newtonian behavior in two ranges, one of no breakdown (low shear stress) and one of breakdown in equilibrium with stresses (high shear stress). In this way, chemical structure is related to physical behavior.

The Temperature Effect

Asphalts are rheologic materials in which the stress-strain characteristics are time dependent. They are also thermoplastic materials with a consistency that varies with temperature. Thus, temperature appears as an independent variable in the rheologic equation of state.

Since climatic variations and construction conditions present a wide range of temperature, the prediction of flow behavior with temperature is of great importance to the asphalt technologist.

The general method used to represent the viscosity-temperature relationship is some form of a graphical plot that produces a straight line relationship for the particular data. Neppe (16) has suggested six possible plots with a description of the equations and their useful temperature ranges.

The viscosity-temperature relationship may be explained structurally by considering conditions within the material at low temperatures. In this state the asphaltenes are precipitated from solution and exist as relatively large associated complexes. As the temperature increases, thermal activity forces the individual molecules farther and farther apart. Since the attractive forces diminish rapidly with distance, the complexes subjected to shear stresses begin to break down and thus the viscosity is reduced. Another contributing factor is that at low temperatures varying amounts of oily constituents are held within the asphaltene complexes by association bonds. As the thermal energy increases, the strength of the bonds decrease and the oils are freed to give

added "lubrication" to the system.

Perhaps the most significant advance in the study of temperature effect is the development of the time-temperature super position principle. This concept was originally developed by the polymeric sciences and was successfully used by Ferry (17) to obtain shear diagrams over a wide range of shear rates. The technique is such that the shear diagrams of a temperature susceptible material like asphalt, determined over a wide range of temperature, are reduced to a common arbitrary temperature. The result is a shear stress-shear rate diagram of the material over a wide range of shear rate at that particular temperature.

The concept, developed originally for analysing creep as a function of time and temperature, separated the two principle independent variables of time and temperature and expressed the mechanical behavior of the material as a single function of time and a single function of temperature. The method was first suggested by Leaderman after observing that creep data taken at different temperatures could be superimposed by horizontal shifts along the log time axis. The origins of the principle, though essentially empirical, can be deduced from flexible-chain theory as explained by Ferry (17).

Viscoelastic response of polymers is the cooperative motion of individual molecular chains and is governed by a friction coeficient, f_o . From Rouse theory, the retardation time is given by Ferry as:

$$t_i = a^2 z^2 f_o / 6\pi^2 i^2 KT \qquad (9)$$

where a is a characteristic dimension of the material, z is the degree of polymerization, i is the integer set 1, 2, 3, ..., n , K is Boltzman's constant, and T is absolute temperature. The temperature dependence enters the above expression in T, a , and f_o , which may be combined into a time reduction factor a_T, the ratio of relaxation times at any temperature and at an arbitrary base temperature, T_o .

$$a_T = \frac{t_T}{t_{T_o}} = \frac{[a^2 f_o]_T}{[a^2 f_o]_{T_o}} \cdot \frac{T_o}{T} \qquad (10)$$

Thus, a change in temperature shifts the complete curve on a log plot by a factor of log a_T. A vertical shift of T_o/T is also made in order to reduce the effects of entropy change to the reference temperature.

Ferry (17), in attempting to find a means of experimentally determining the shift factor, used the relationship:

$$a_T = \frac{\eta T_o \rho_o}{\eta_o T \rho} \qquad (11)$$

where η and η_o are measured viscosities at T and T_o respectively, and ρ and ρ_o are densities at the corresponding temperatures. Therefore, if the temperature dependence of the viscosity is known, it is no longer necessary to obtain a_T empirically.

To have equivalence in effect of time-temperature indicates that all molecular processes occurring on deformation of the material must be retarded or accelerated by the same amount with a temperature change. Thus, the apparent energy of activation, ΔE , is the same for all processes. Then, using an Arrhenius equation:

$$\eta = A e^{\Delta E/RT} \qquad (12)$$

where R is the universal gas constant, and ΔE and A can be considered constants over limited temperature ranges. ΔE can be evaluated as the slope of the straight line of log viscosity versus reciprocal test temperature where viscosity is compared at a constant shear rate, shear stress, or power input. Combining equations (11) and (12) gives:

$$a_T = \frac{\eta T_o}{\eta T} = \frac{T_o}{T} e^{\frac{\Delta E}{R}\left(\frac{1}{T} - \frac{1}{T_o}\right)} \qquad (13)$$

Therefore, if the apparent energy of activation is constant, the values of the shift factor, a_T , may be

calculated at any temperature. This a_T may then be used to accomplish a shift in the temperature domain of any temperature dependent parameter of asphalt flow.

PURPOSE AND SCOPE

Purpose

It is the purpose of this study to investigate the rheologic properties of asphalt cements used as binders in highway pavements, and to determine the applicability of various flow models, especially the hyberbolic sine model, to the prediction of asphalt flow characteristics over wide ranges of shear rate and temperature. Furthermore, studies of various models to explain the effect of temperature on the asphalts, with particular attention to thermodynamic analysis, are made.

To accomplish this, viscosity data is taken for asphalts of different flow characteristics. In order to extend the workable ranges of shear rate and temperature, several viscometers of different types are used. By this method, data are taken for a temperature range of $-10^{o}C$ to $160^{o}C$ and for a shear rate range of 10^{-4} reciprocal seconds to 10^{4} reciprocal seconds. A computer program is used to evaluate the parameters of the hyperbolic sine model. The results are critically analysed and compared with prior work. Possible explanations for observed error are given. The flow data are analysed using thermodynamic techniques in order to explain viscosity change with changing temperature.

MATERIALS AND PROCEDURE

Materials

The three asphalts used in this study are a 60-70 penetration grade asphalt cement from a Venezualan crude, an AC-20 grade asphalt cement coded B-3056, and an AC-20 grade asphalt cement coded B-2960. The latter two were used in the "Asphalt Institute-Bureau of Public Roads Cooperative Study of Viscosity-Graded Asphalts." The results of conventional tests on the asphalts are shown in table 1.

Sliding Plate Microviscometers

A sliding plate microviscometer, made by Hallikainen Instruments, and a Varian Model G-14 graphic recorder were used to obtain viscosity data in a shear rate range of 10^{-4} to 10^{0} reciprocal seconds, and in a temperature range of $5^{o}C$ to $60^{o}C$. Specimen preparation and testing were done following ASTM (Proposed Method of Test for Aging Index of Bituminous Materials, 1964). Total deformation was limited to 200 microns of plate movement on any one specimen. Film thicknesses of 30 to 80 microns were used between glass plates of 6 cm^2 area.

A second sliding plate apparatus using an Instron testing machine to shear stainless steel plates of

Table 1- The Results of Conventional Tests on Asphalts Used in this Study.

Test	Asphalt Type		
	60-70	B-3056	B-2960
Specific Gravity 77/77°F	1.010	1.020	1.034
Softening Point, Ring and Ball	123°F	---	125°F
Ductility 77°F	150+cm	250+cm	---
Penetration 100gm, 5 sec, 77°F	63	---	---
Penetration 200gm,60 sec, 39.4°F	23.5	30	---
Flash Point, Cleveland Open Cup	455°F	545°F	515°F

1.2 cm^2 area at a constant rate also was used. This setup gave a shear rate range of 10^{-3} to 10^{-1} reciprocal seconds, and a temperature range of -10°C to 5°C. The calculation procedure for both of these instruments is relatively simple as the geometry of the samples is the same as that used to define viscosity. The data was, therefore, used with no corrections for either Newtonian or Non-Newtonian flow.

Capillary Viscometers

Capillary tests were run with Cannon-Manning vacuum viscometers using the Cannon vacuum regulator and a model H-1 high temperature oil bath. Accuracy was maintained to $\pm$0.5mm Hg for a range of 5 to 50mm Hg, and to $\pm$0.01°C for a range of 45°C to 160°C, test temperature. The geometry of the viscometers is described in detail elsewhere (18). Testing was carried out in accordance with ASTM (Tentative Method of Test for Absolute Viscosity of Asphalt, D 2171-63T). By using different sized viscometers and different degrees of vacuum it was possible to get a shear rate range of one decade in reciprocal seconds at any one temperature. Three tests were run to describe this range. Data calculation was again simple as upon checking the error due to non-Newtonian flow as described by Brodkey (19), it was found

that the effect was negligible.

Rotational Viscometer

The fourth instrument used was a Haake Rotovisco connected to the Varian G-14 recorder. This instrument was used for testing in the 45°C to 160°C temperature range at low shear rates, and its test procedure is well described by Van Wazer et al. (18). Briefly the Rotovisco consists of a control unit and a measuring head, which are connected mechanically and electrically by a flexible shaft. The sample is introduced into a gap between two coaxial cylinders which are surrounded by an oil jacket heated to within $\pm$0.1°C of the test temperature. A drive motor, through a multiple speed transmission, causes the inner cylinder to rotate. An electrical torsion dynamometer, consisting of two coaxial shafts mechanically coupled by a creep-resistant torsion spring, measures the angular displacement of the spring caused by the torque on the cylinder immersed in the test material. This torque is then a measure of the viscosity.

RESULTS AND DISCUSSION OF RESULTS

In this section the results of rheologic testing are presented and discussed. The order of presentation is; consistency and calculation of data, the flow diagram, the temperature effect, thermodynamic concepts, and the hyperbolic sine.

Consistency and Calculation of Data

Flow data were obtained using capillary, sliding plate, and rotational viscometers. Each instrument could be used only for a certain range of temperature, shear rate and shear stress. Figure 3 shows data taken at 45°C for which it was possible to use all but the Instron-sliding plate viscometer. This plot of log viscosity versus log shear rate for the 60-70 asphalt shows that the instruments gave overlapping data, and that the data were continuous. The slight deviation at low shear rates for the sliding plate viscometer was caused by inaccuracies in transmitting very low stresses to the specimens.

The calculation of data for the capillary and rotational viscometers was based on Newtonian flow. In order to determine the viscosity of non-Newtonian materials, some corrections were necessary. Following the procedure suggested by Brodkey (19), it was found that for the test temperatures used in this study, the

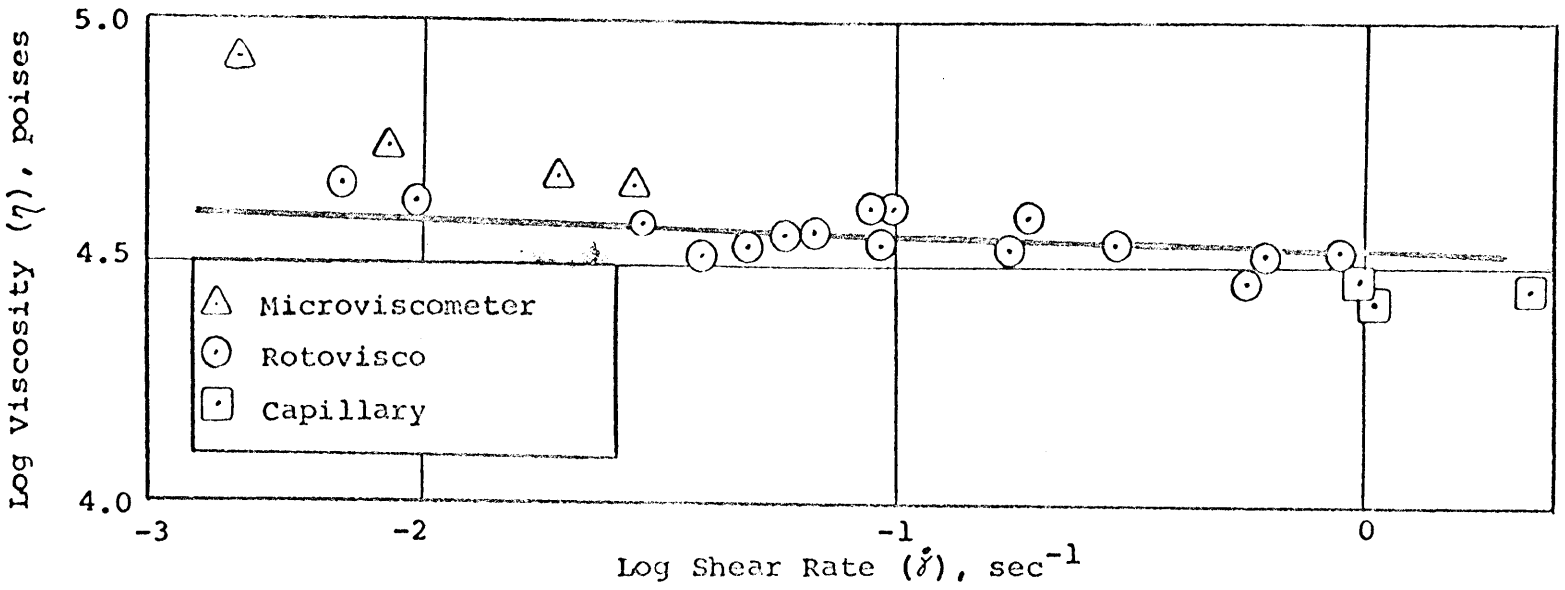

Figure 3 - Viscosity versus Shear Rate for 60-70 Penetration Grade Asphalt at 45°C with Three Different Viscometers.

data could be treated as Newtonian.

To facilitate the examination and analysis of data, and to reduce experimental variations, smooth curves were drawn through the experimental data points. From these best fit curves, a series of three to five new data points were taken and tabulated in Appendix I for the three asphalts at all the test temperatures.

Flow Diagram

To show the relative consistency differences among the three asphalts used in this study, arithmetric plots of shear rate versus shear stress were constructed for various test temperatures in figures 4, 5, and 6. A comparison shows that the three asphalts, for the range of shear rates and test temperatures used in this study, are Newtonian for temperatures above 45°C. At temperatures below 45°C all three asphalts exhibit a certain degree of non-Newtonian behavior with the B-3056 asphalt being the most non-Newtonian and the 60-70 asphalt being the least.

As a first step in establishing a flow model for the asphalts, figures 7, 8, and 9, the log shear rate versus log shear stress diagrams, were constructed. In general the data produced straight lines, and a

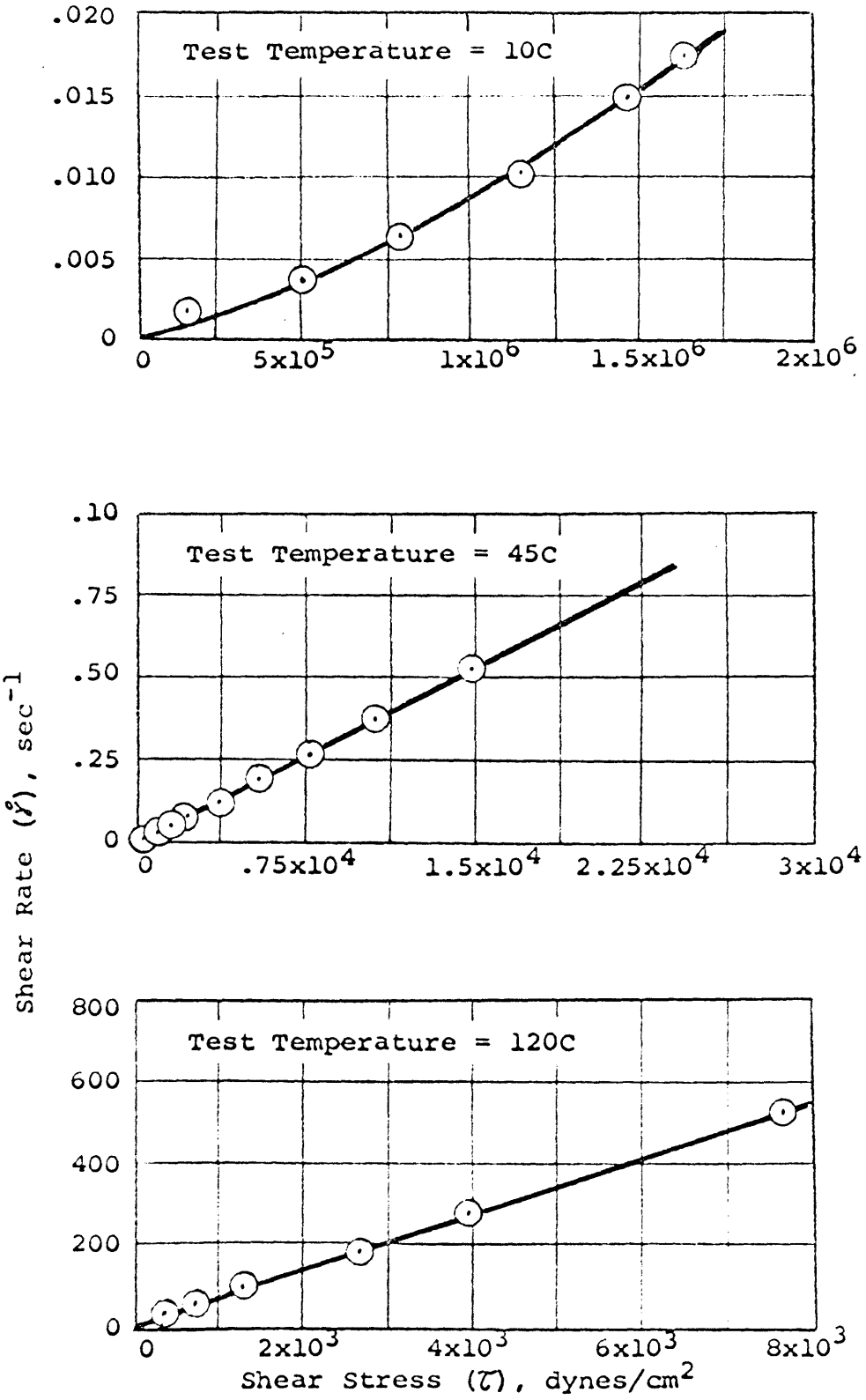

Figure 4 - Shear Rate versus Shear Stress on Arithmetic Scales for the 60-70 Asphalt at Various Test Temperatures.

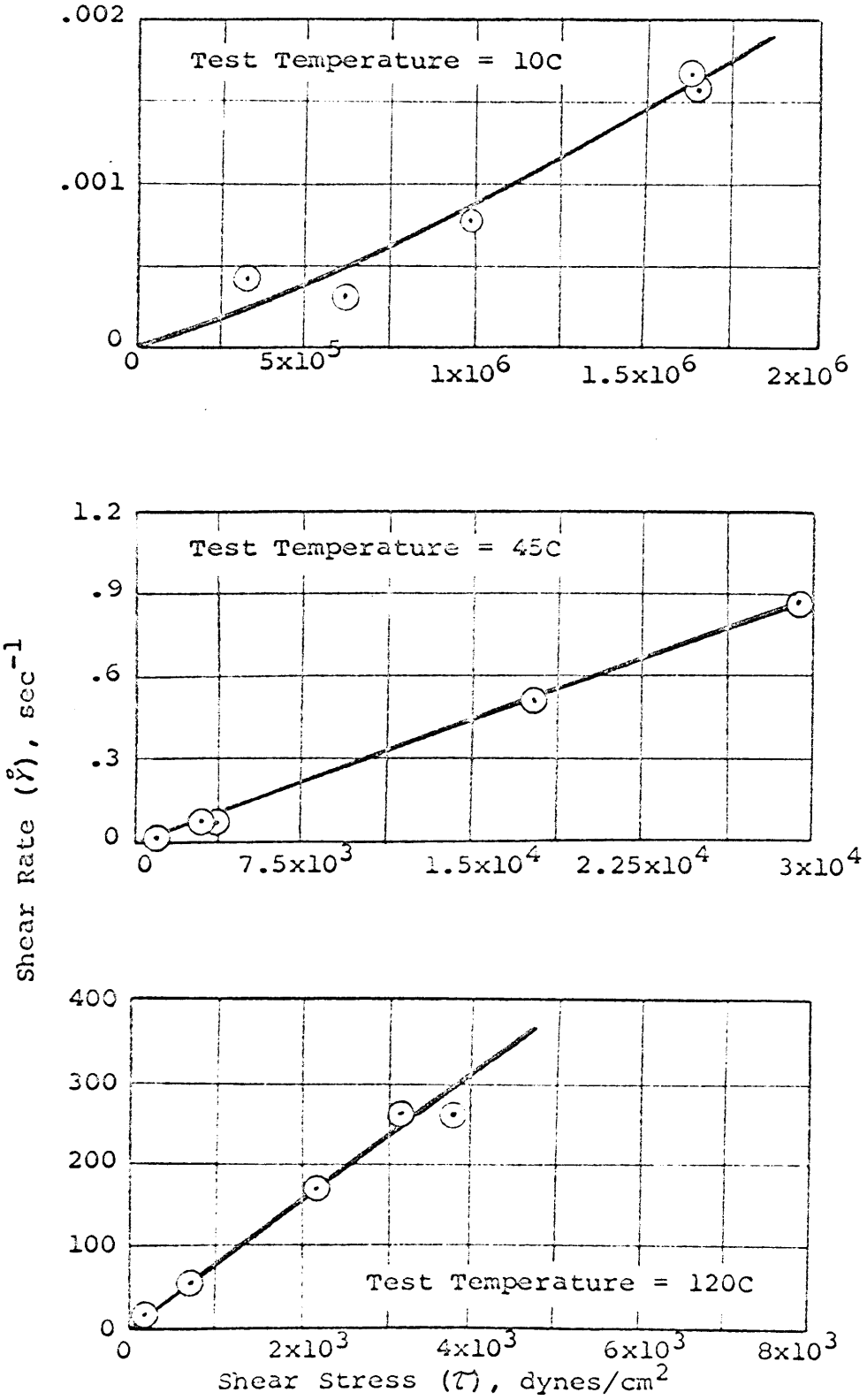

Figure 5 - Shear Rate versus Shear Stress on Arithmetic Scales for the B-3056 Asphalt at Various Test Temperatures.

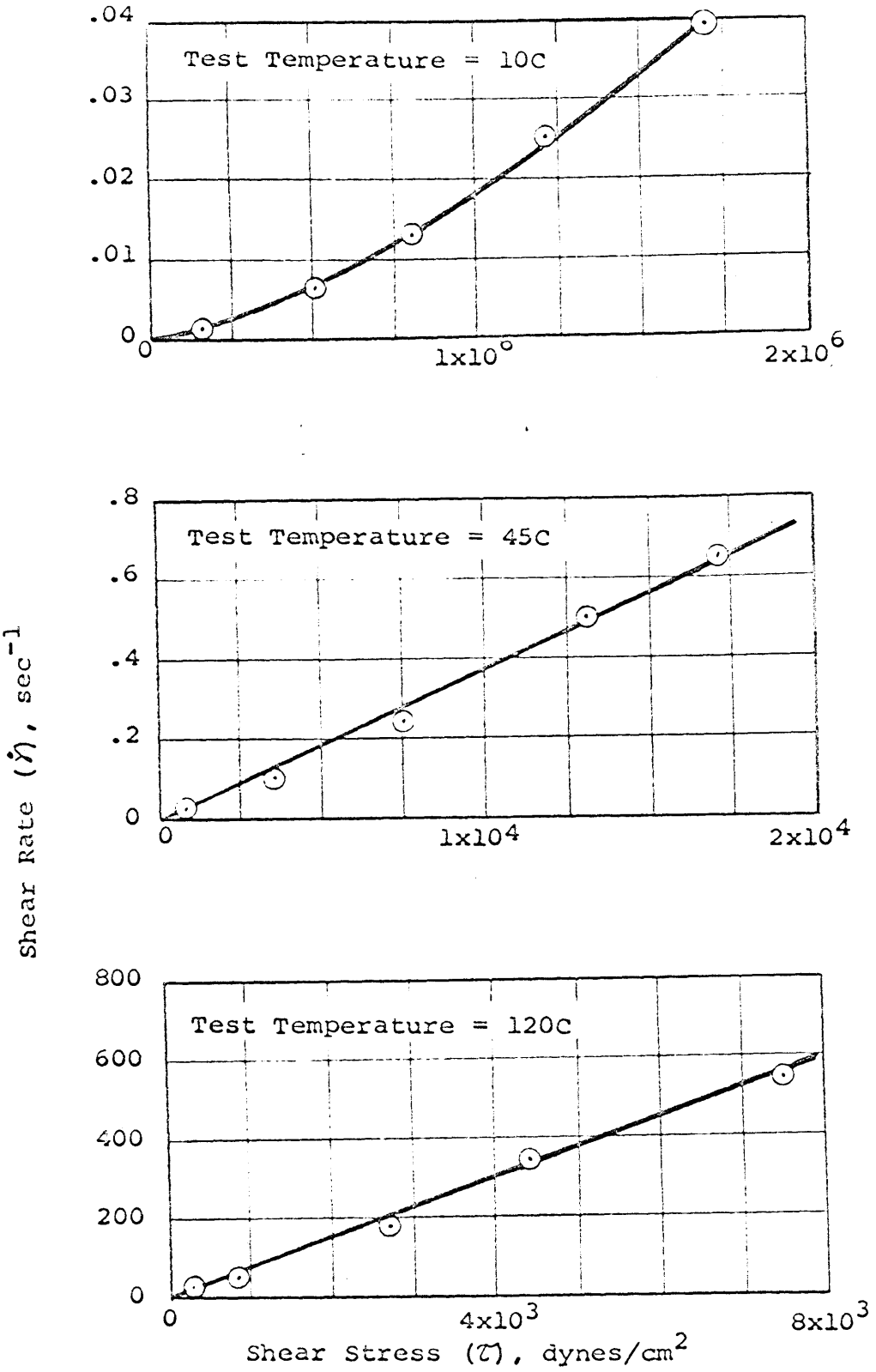

Figure 6 - Shear Rate versus Shear Stress on Arithmetic Scales for the B-2960 Asphalt of Various Test Temperatures.

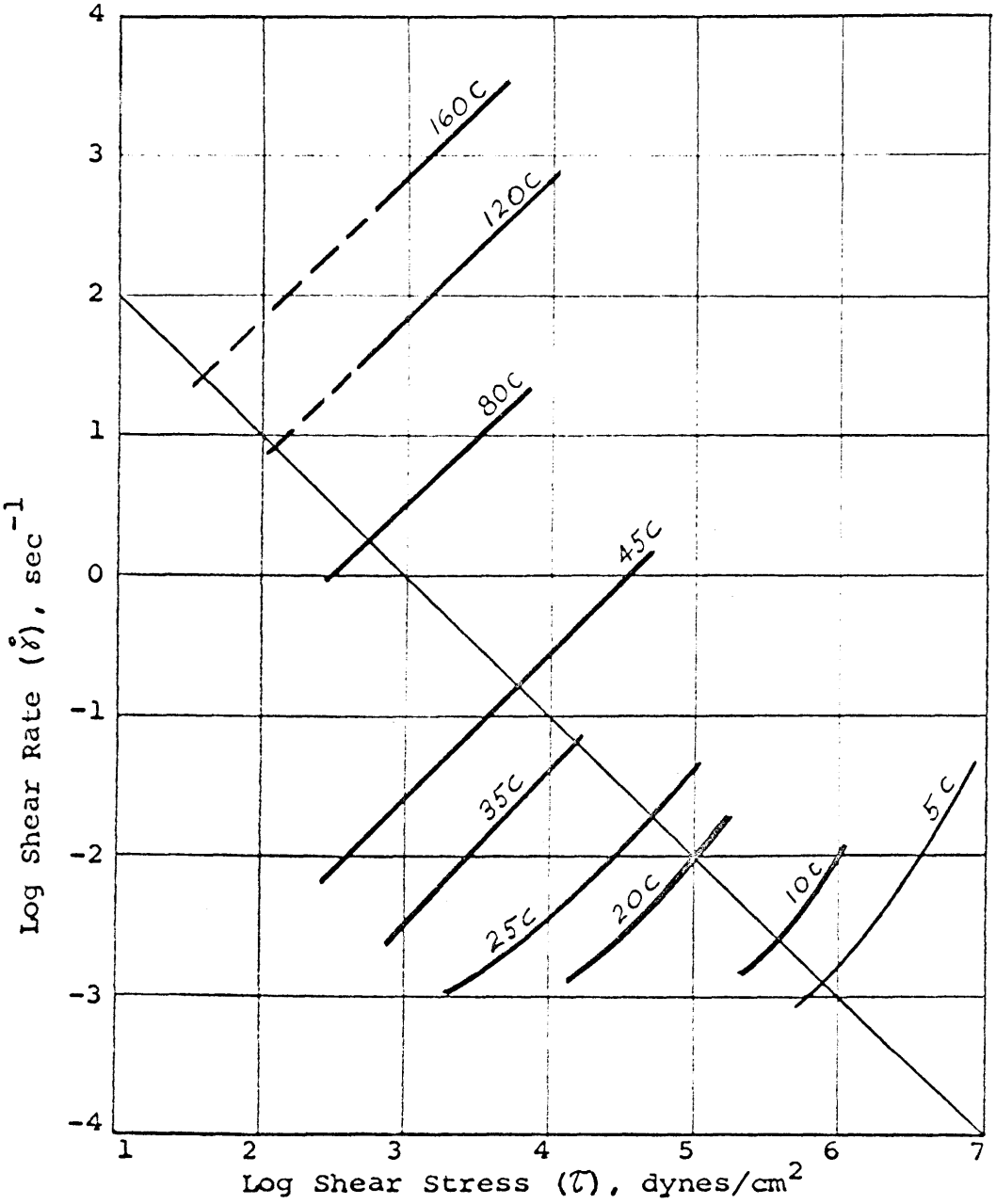

Figure 7 - Shear Rate versus Shear Stress on Log-Log Scales for the 60-70 Penetration Grade Asphalt at All Test Temperatures.

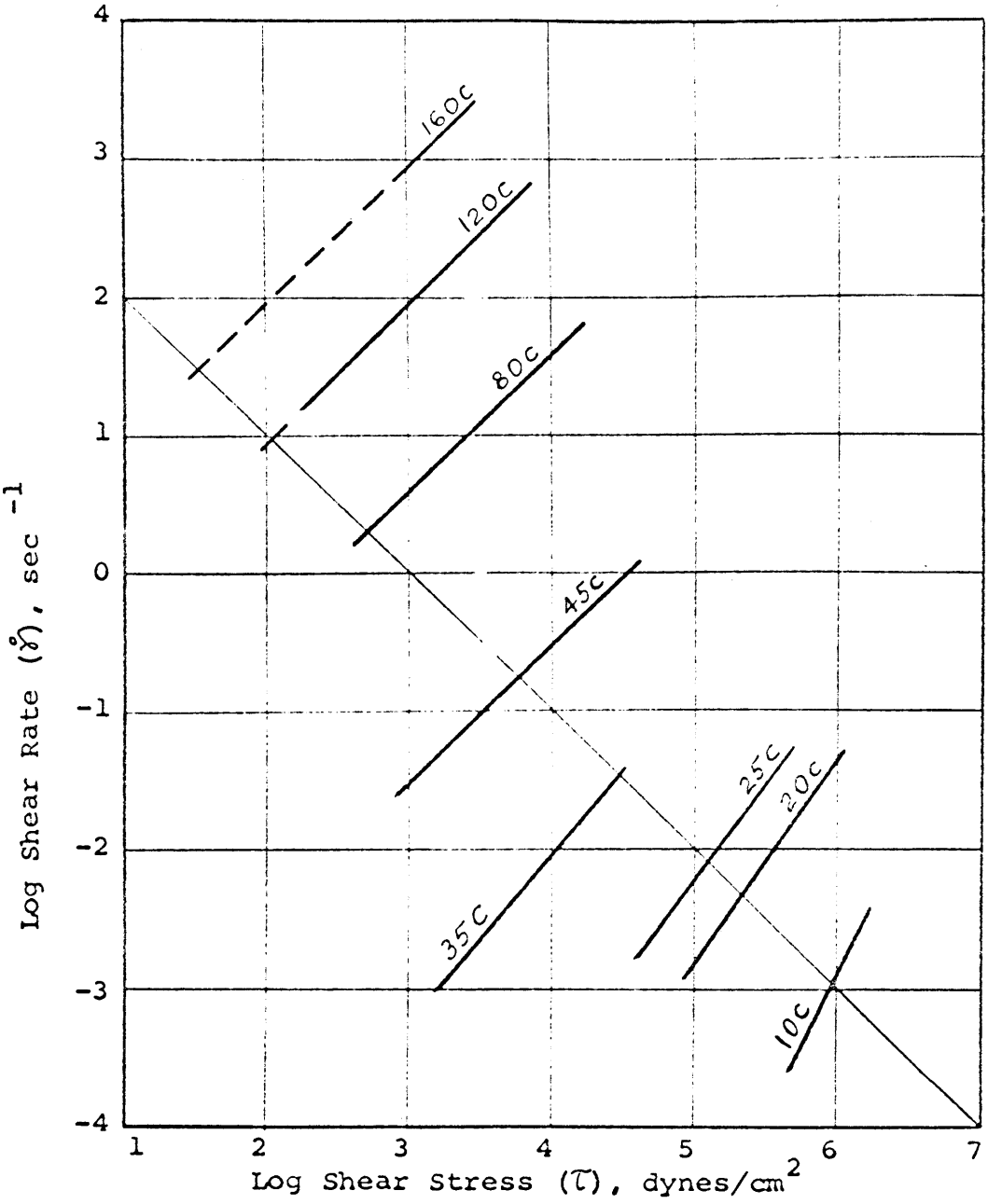

Figure 8 - Shear Rate versus Shear Stress on Log-Log Scales for the B-3056 Asphalt at All Test Temperatures.

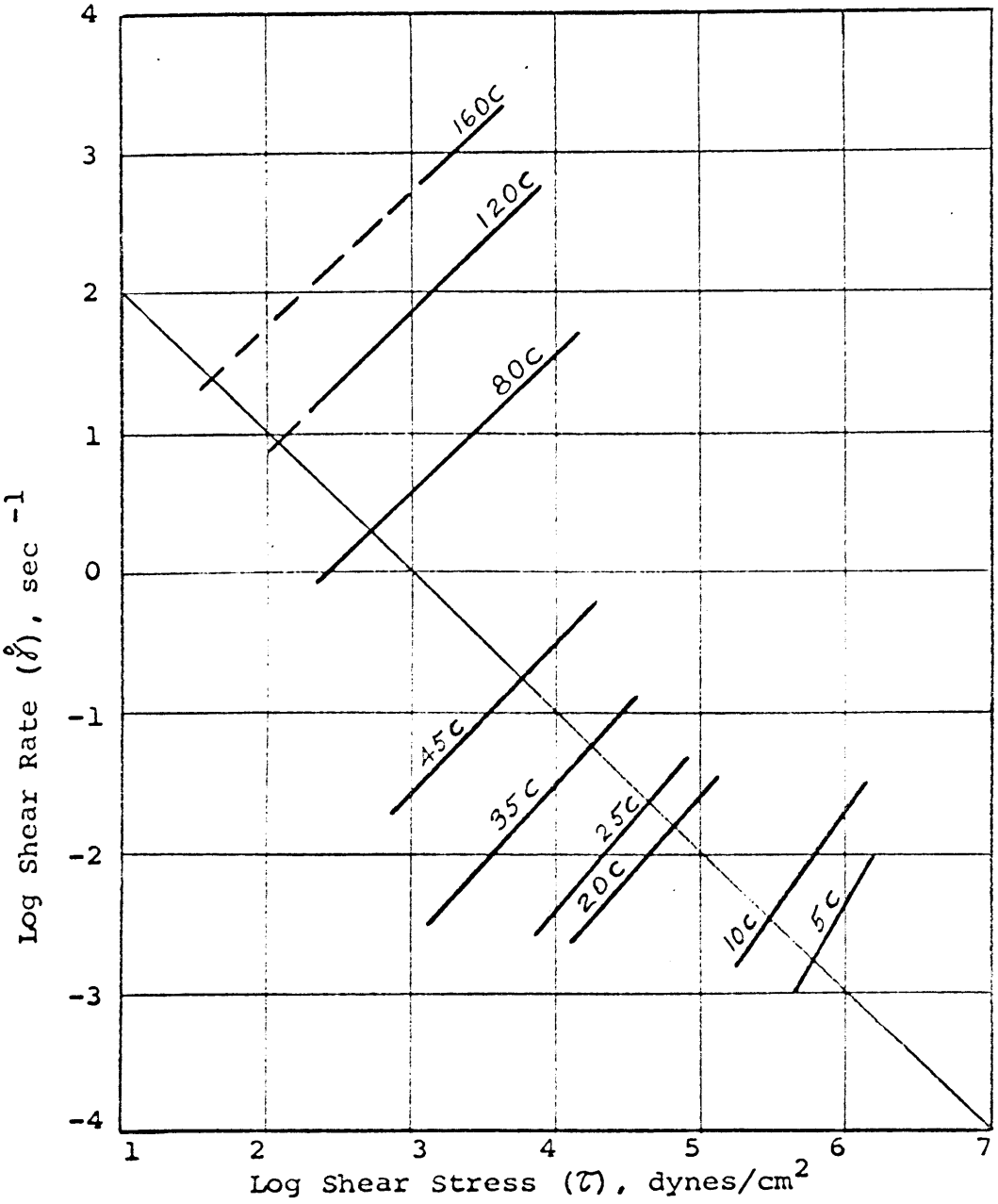

Figure 9 - Shear Rate versus Shear Stress on Log-Log Scales for the B-2960 Asphalt at All Test Temperatures.

power function of the type:

$$\tau = A(\dot{\gamma})^n \qquad (14)$$

could be used to represent the flow behavior of these asphalts where n, the slope of the curves, is an indication of the non-Newtonian behavior. As n deviates from unity (the Newtonian case) the flow behavior becomes more non-Newtonian. Figures 7, 8, and 9 show that at 45°C and lower, among the three asphalts, the B-3056 material is the most non-Newtonian in flow behavior. It has the lowest value of slope, n, while the slope for the 60-70 asphalt is the closest to unity.

Using the alternative flow diagram, log viscosity versus log shear rate, figures 10, 11, and 12 were constructed. These figures show that the data, in general, produce straight lines, and that the flow behavior may be represented by the power function:

$$\eta_a = A(\dot{\gamma})^{n-1} \qquad (15)$$

which agrees with the previous model assumed for these materials. For this plot, Newtonian flow is represented by a horizontal line, and for the three asphalts shown, the results above 45°C produced horizontal lines. The B-3056 asphalt has the greatest negative slopes in the non-Newtonian range in agreement with the fact that it

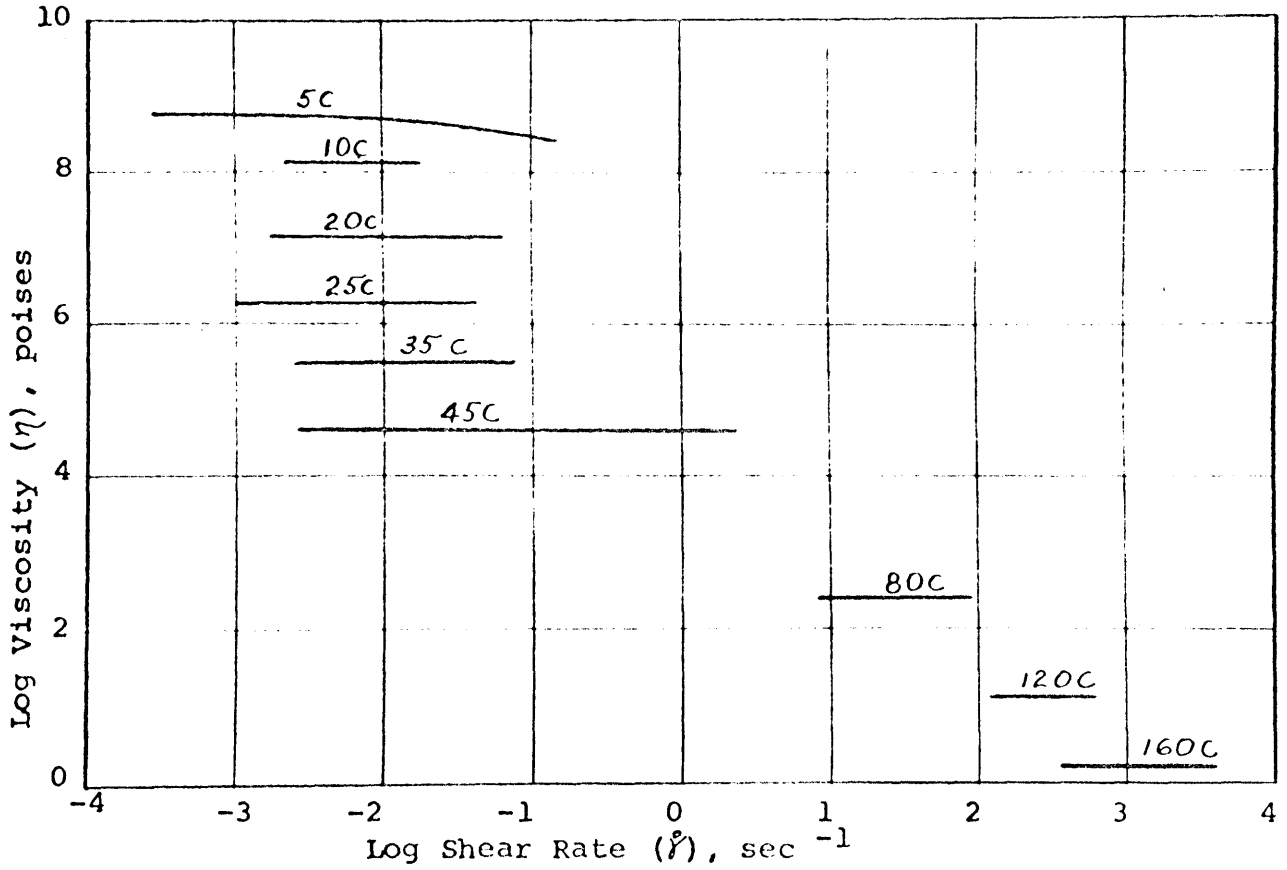

Figure 10 - Viscosity versus Shear Rate for the 60-70 Penetration Grade Asphalt at All Test Temperatures.

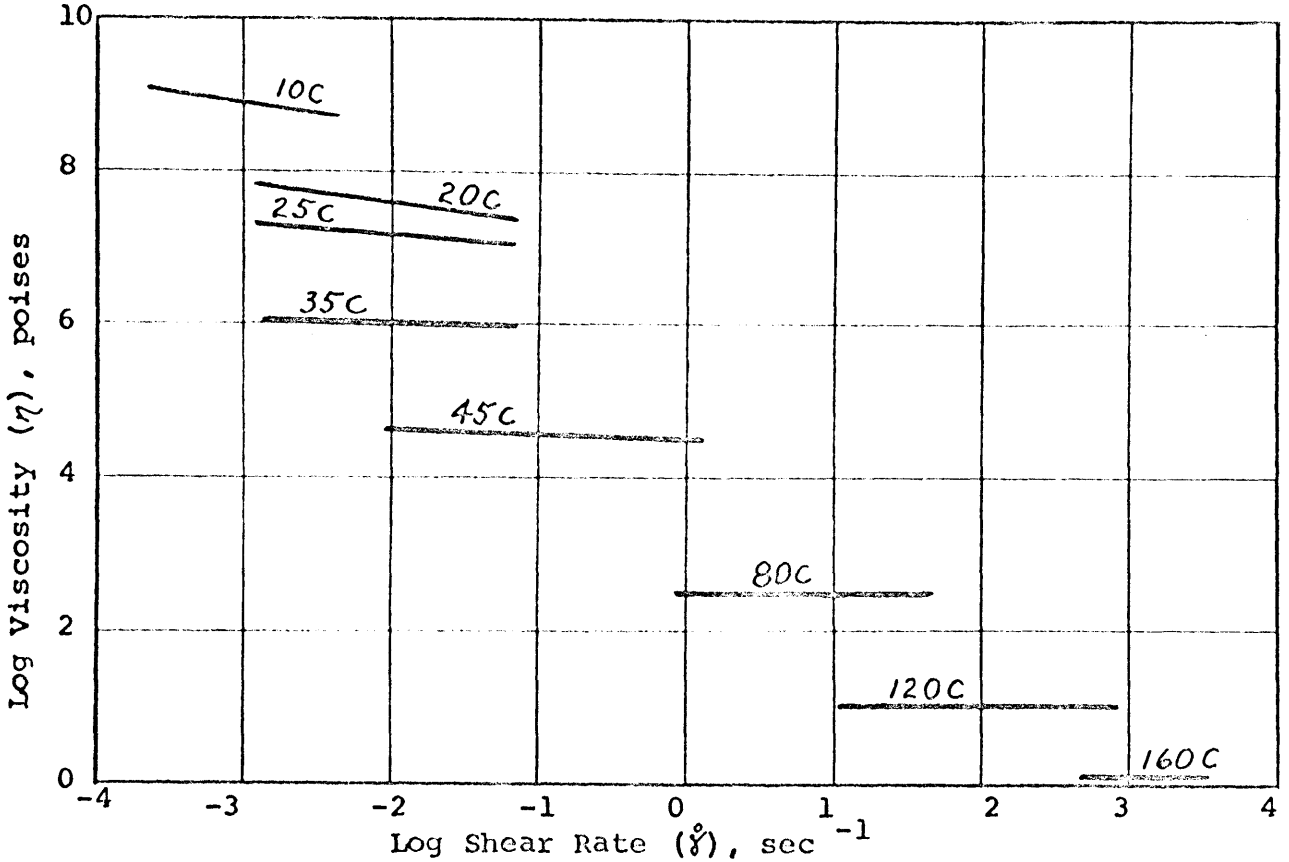

Figure 11 - Viscosity versus Shear Rate for the B-3056 Asphalt at All Test Temperatures.

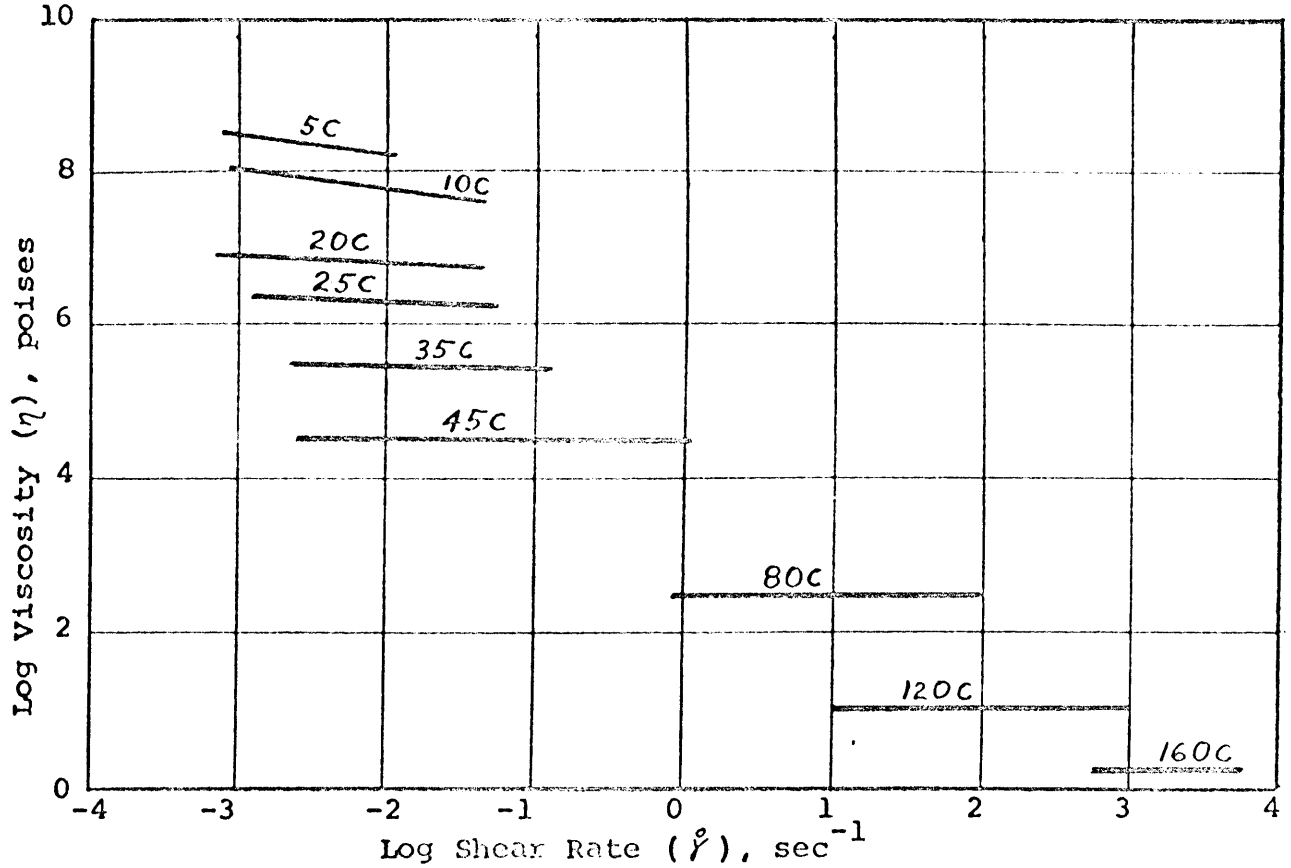

Figure 12 - Viscosity versus Shear Rate for the B-2960 Asphalt at All Test Temperatures.

is the most non-Newtonian of the three asphalts. The 60-70 asphalt displays very nearly Newtonian behavior over the entire range of test temperatures.

Figures 13 and 14 are plots of log viscosity versus log shear stress for the 60-70 and B-3056 asphalts respectively. The generally straight lines again suggest a power function of the form:

$$\eta_a = A(\tau)^{1-n} \qquad (16)$$

As with previous figures of log viscosity versus log shear rate, Newtonian flow behavior is characterized by a horizontal line as shown by the results for temperatures above 45°C.

For Newtonian materials, viscosity is independent of shear stress and shear rate, and is constant at any one temperature. For such a material the relationship describing the temperature dependency of viscosity is independent of shear rate and shear stress, and can be expressed satisfactorily by the Arrhenius equation:

$$\eta = A \exp(\Delta E/RT) \qquad (17)$$

where R is the universal gas constant, and A and ΔE can be considered as constants over limited temperature

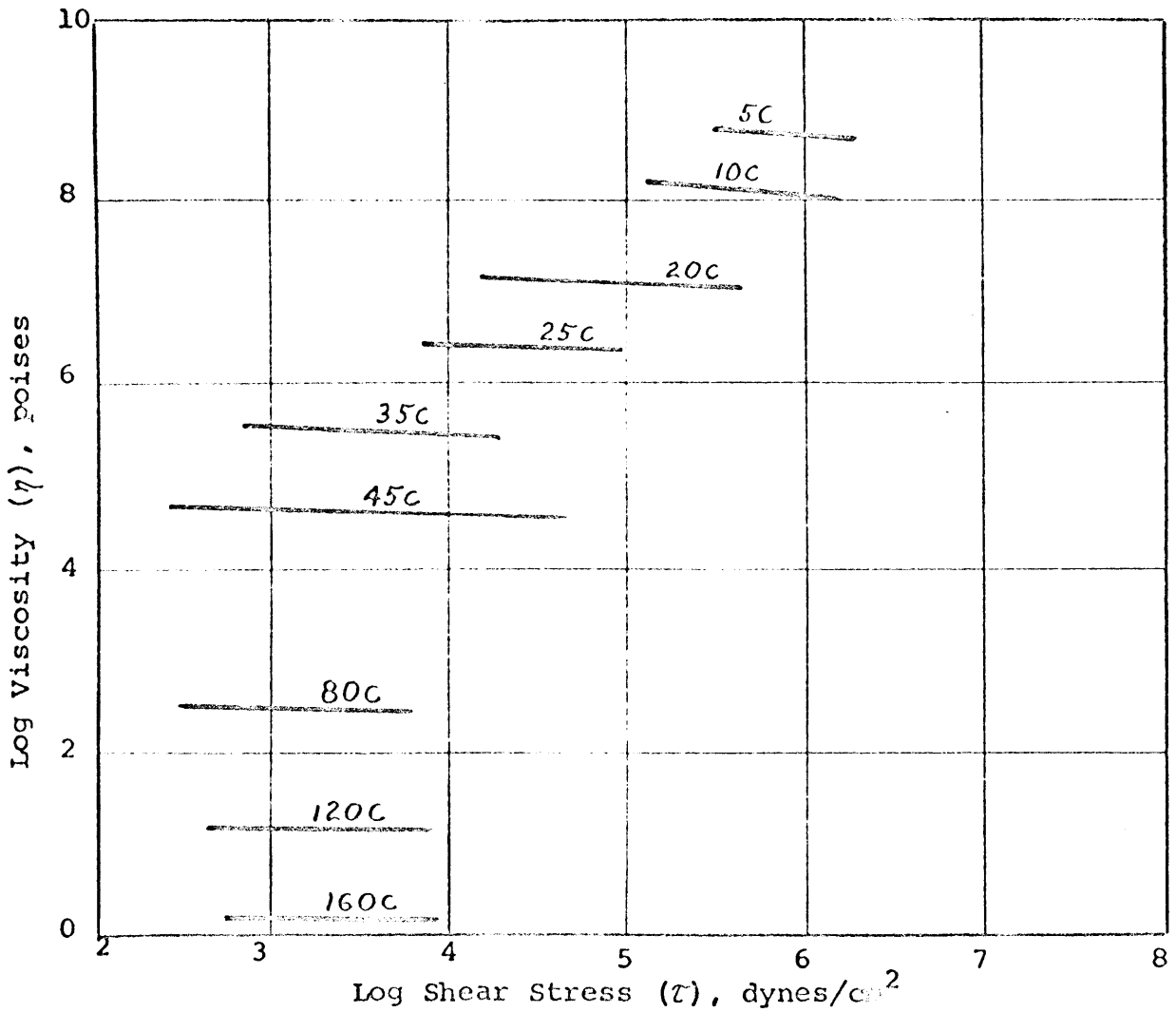

Figure 13 - Viscosity versus Shear Stress for the 60-70 Penetration Grade Asphalt at all Test Temperatures.

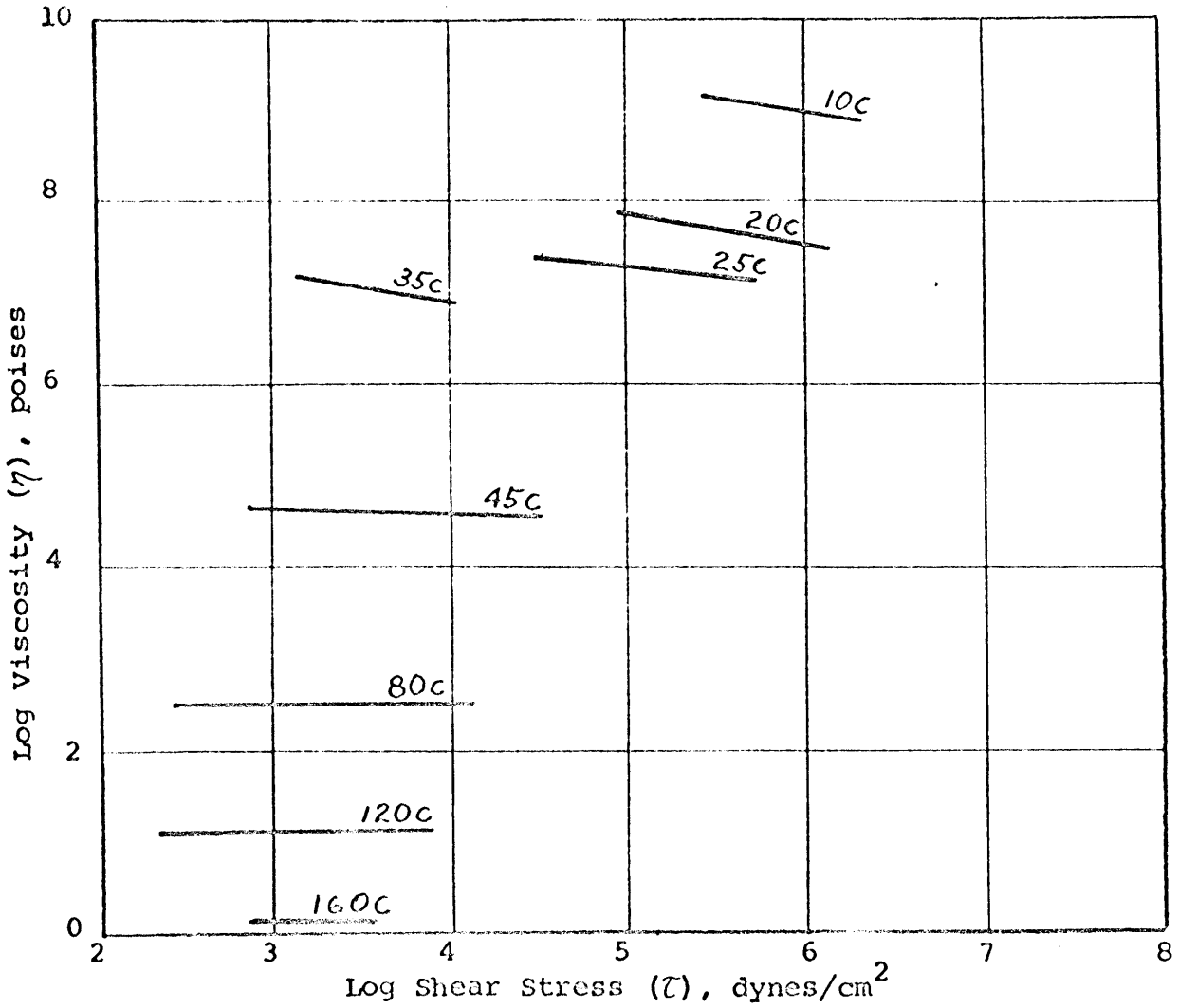

Figure 14 - Viscosity versus Shear Stress for the B-3056 Asphalt at All Test Temperatures.

ranges.

For non-Newtonian materials, however, the viscosity at a fixed temperature is dependent on shear stress or shear rate. Therefore, in order to develop an expression like equation (17) to represent the temperature dependency, either A or ΔE or both must be considered functions of shear stress or shear rate.

At fixed shear rate, the viscosity can be expressed as:

$$\eta(\dot{\gamma}, T) = \frac{\tau(\dot{\gamma}, T)}{\dot{\gamma}} \qquad (18)$$

and at fixed shear stress as:

$$\eta(\tau, T) = \frac{\tau}{\dot{\gamma}(\tau, T)} \qquad (19)$$

Formal differentiation of these two equations with respect to temperature at fixed shear stress and at fixed shear rate respectively results in (20):

$$\frac{(\partial\eta/\partial T)_{\dot{\gamma}}}{(\partial\eta/\partial T)_{\tau}} = \left(\frac{\partial \ln \eta}{\partial \ln \dot{\gamma}}\right)_T + 1 \qquad (20)$$

and

$$\frac{(\partial\eta/\partial T)_{\tau}}{(\partial\eta/\partial T)_{\dot{\gamma}}} = 1 - \dot{\gamma}\left(\frac{\partial\eta}{\partial\tau}\right)_T \qquad (21)$$

For materials such as asphalt which show a decrease in viscosity with an increase in shear rate or shear stress or both, $(\partial\eta/\partial\tau)_T$ and $(\partial \ln \eta/\partial \ln \dot{\gamma})_T$ are negative. Therefore, the $(\partial\eta/\partial T)_{\tau}/(\partial\eta/\partial T)_{\dot{\gamma}}$ is

larger than or equal to one. This indicates that the temperature variation of viscosity at fixed shear stress is greater than the variation at fixed shear rate. In figures 7, 8, and 9 the viscosity variation at fixed shear stress is obtained using a vertical cress plot, and the corresponding variation with fixed shear rate is obtained using a horizontal cross plot. Since the slopes of the lines in these figures are always greater than or equal to one for these three asphalts, the variation of viscosity with shear stress is greater than the variation with shear rate.

Temperature Effect

To observe the effect of temperature on asphalt, a suitable method of choosing comparable viscosities must be found. A method of representation must be used such that some model will represent the data, and that the model will have some physical meaning. For the data obtained in this study, the comparison of viscosities at different test temperatures for fixed shear stresses or shear rates would necessitate excessive extrapolation at either extreme of temperature. The method of constant power input, although rather arbitrary in nature, does offer the advantage that very little extrapolation is necessary. Consequently this

method was used, and a constant power input of 1000 $(\tau \times \dot{\gamma})$ per unit volume was chosen as convenient.

The most suitable method of representing the viscosity-temperature change for these three asphalts was to plot the log viscosity, as determined by a constant power input, versus the reciprocal of the absolute test temperature as shown by the curves in figure 15.

For all three curves, the viscosity-temperature relationship is two straight lines intersecting at a point near the ring and ball softening point of each asphalt. Then, except for the small range of temperature around the softening point, the temperature dependency of viscosity may be represented by equation (17) where the slope $\Delta E/R$ is different above and below the softening point, but constant in each range.

The curved portion of the viscosity-temperature curve denotes some relatively rapid physical change in the flow behavior of the asphalts. Traxler and Schweyer (21), noticing similar behavior, attributed this change in slope near the softening point to the colloidal nature of the asphalt. They suggested that the colloidal structure of the asphalt changes more rapidly with temperature in this region than in other temperature regions. This would result in a difference

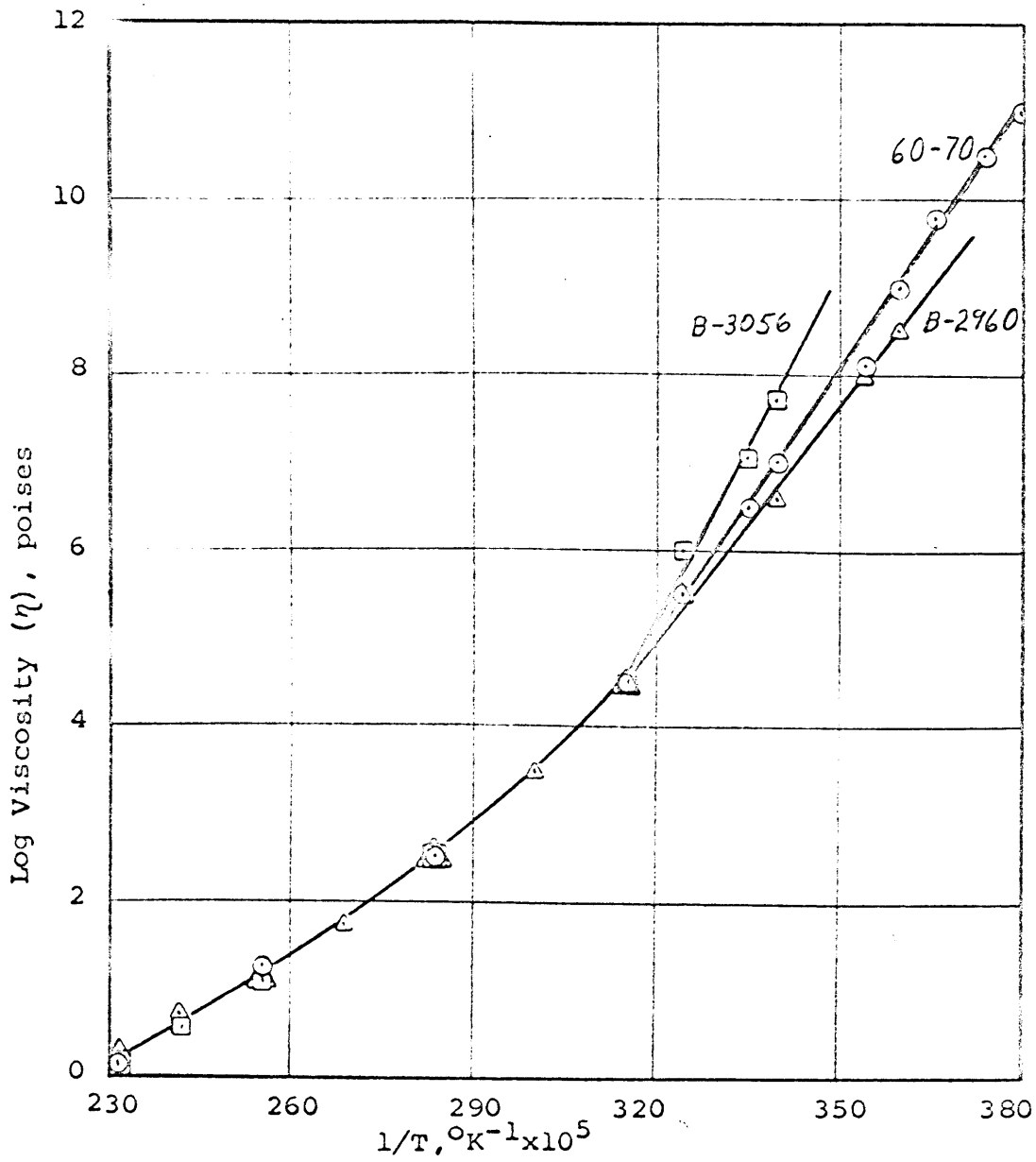

Figure 15 - Viscosity versus Reciprocal Absolute Test Temperature for All Asphalts.

in the temperature susceptibility of the material in that region.

Since, under ordinary pavement conditions, an asphaltic binder could be subject to very low shear rates such as thermal expansion and contraction, and to very high shear rates such as during the compaction process, it would be very useful to establish the flow diagram of an asphalt over a much wider range of shear rate than was possible with the instruments used in this study. Using Ferry's (17) principle of reduced variables, it would be desirable to transform from the test temperature parameter to the shear stress parameter.

Although the base temperature in equation (11) is an arbitrary choice, the best accuracy can be obtained using a temperature midway in the span of data to be reduced. Figures 7, 8, and 9 show that a base temperature of $45^{o}C$ $(318\,^{o}K)$ would be most suitable.

Noting that the apparent viscosity is shear stress divided by shear rate, and that the term ρ_o/ρ is usually disregarded as negligible, the shift factors, a_T, could be calculated from a form of equation (11) as:

$$a_T = \frac{\tau}{\tau_o} \frac{\dot{\gamma}_o}{\dot{\gamma}} \frac{T_o}{T} \qquad (22)$$

In order to construct the master flow curves, a

series of data points (in this case two or three) for each test temperature from the original flow diagrams (figures 7, 8, and 9) were multiplied or divided by their respective a_T's and reploted as shown in figures 16, 17, and 18. These figures show that master curves can be constructed covering approximately seven logrithmic decades of shear rate when the data is treated as outlined above. A comparison of the three curves shows that all three asphalts have almost identical master curves. Because the shift was performed along the shear stress axis, the coincidence of the curves shows that the asphalts had essentially the same susceptibility to shear stress, and that the difference in their flow behavior is due to differences in their shear rate susceptibility.

Thermodynamic Analysis

Thermodynamic parameters, derived from analysis of asphalt flow behavior, can be used for the comparison of different asphalts, to transfer and extend limited data, and to provide a useful method of testing various rational theories of fluid flow.

One approach to thermodynamic analysis considers equation (17) as developed for the curves in figure 15. Dividing each curve at the point of curvature into two

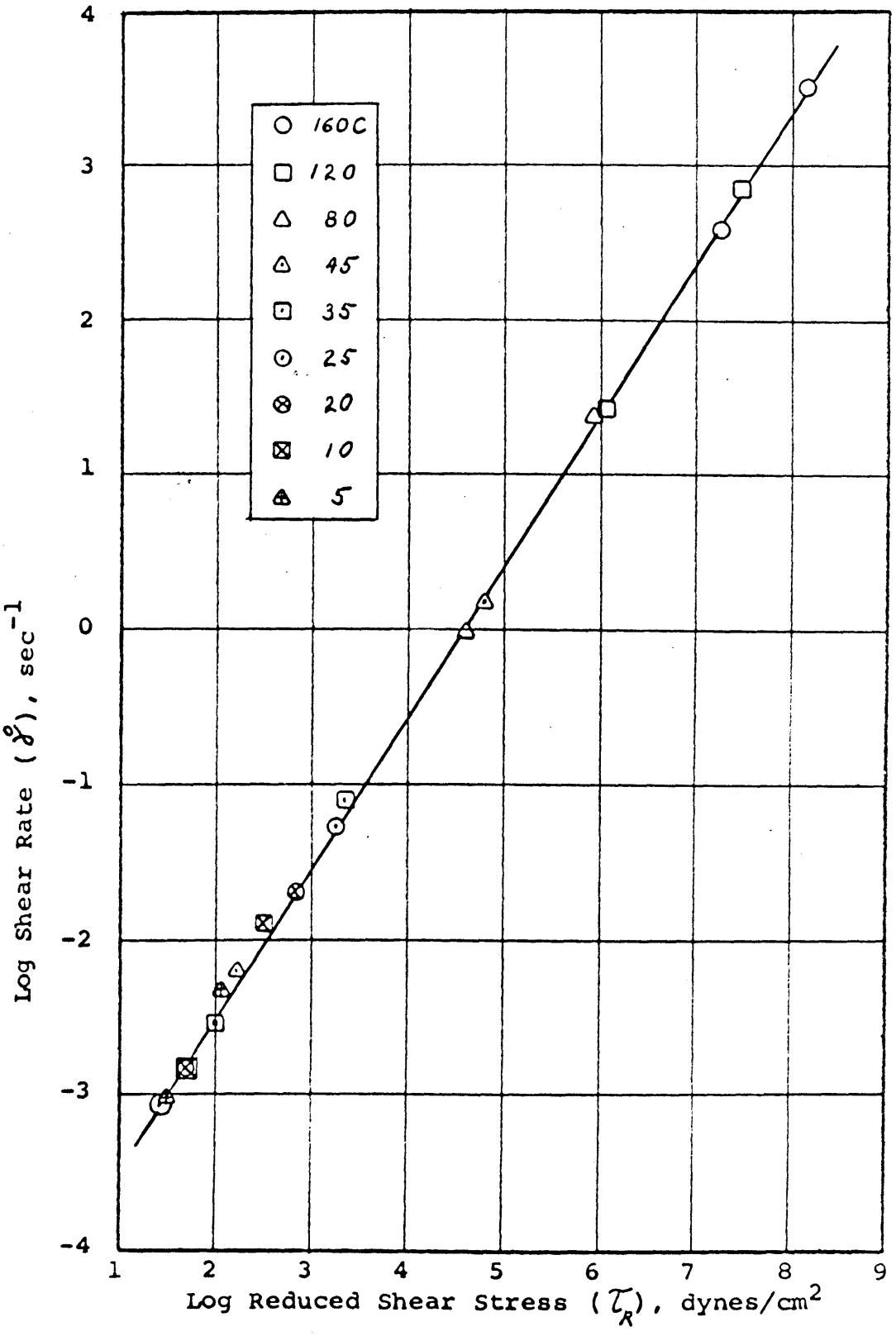

Figure 16 - Master Flow Diagram for the 60-70 Asphalt.

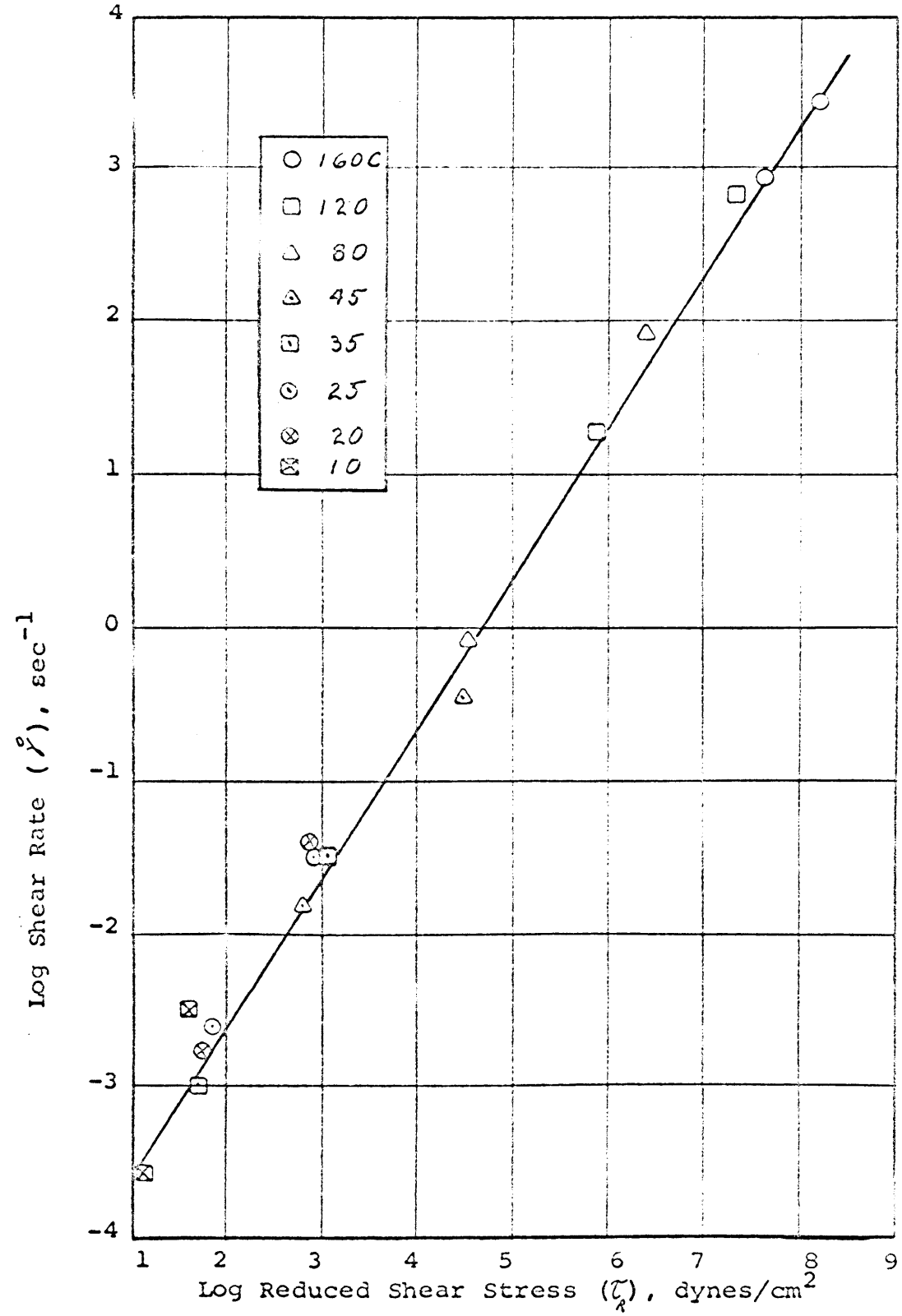

Figure 17 - Master Flow Diagram for the B-3056 Asphalt.

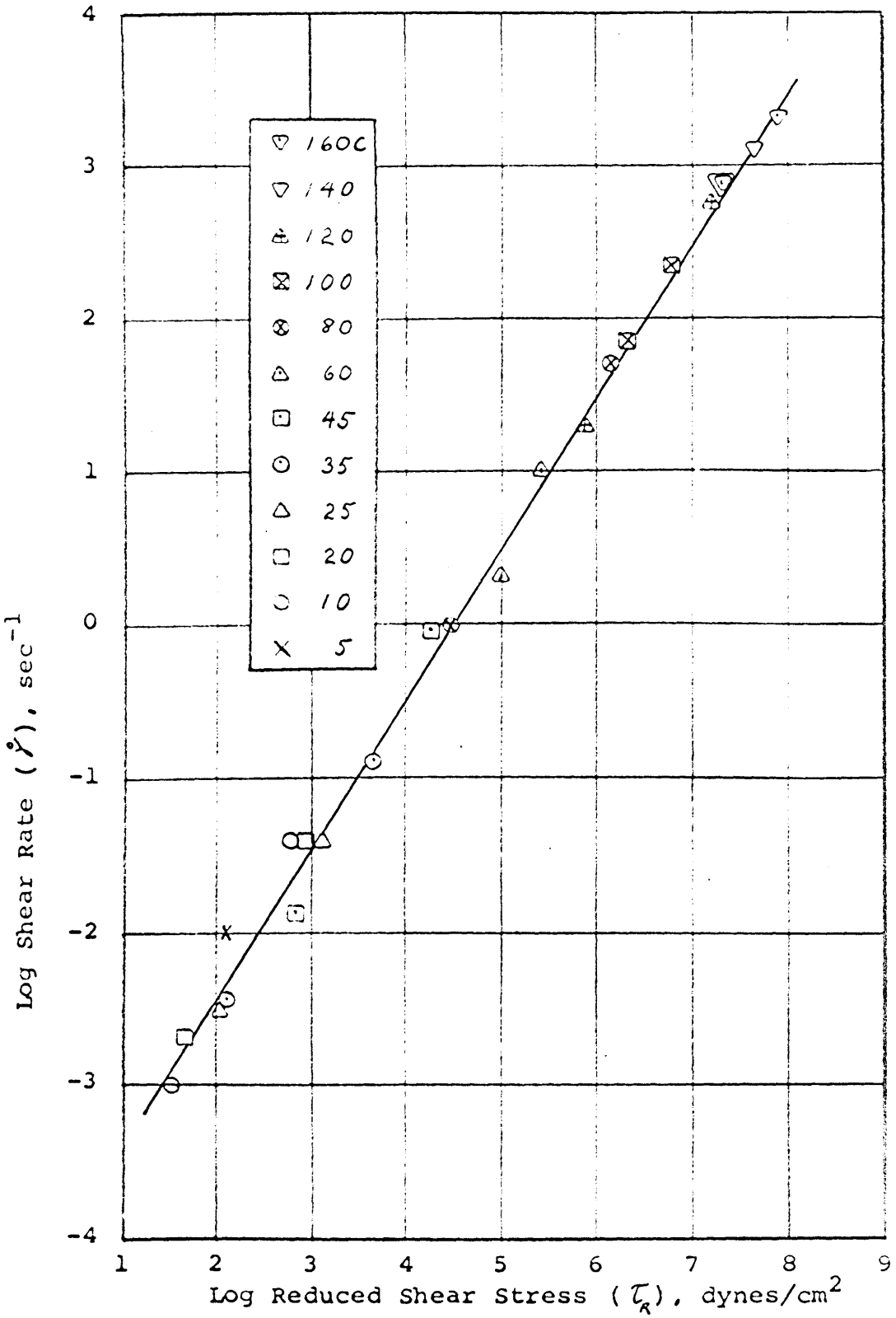

Figure 18 - Master Flow Diagram for the B-2960 Asphalt.

segments gives two models of the flow behavior:

$$\eta_a = A' \exp(\Delta E'/RT) \quad , \quad T > \text{softening pt.} \qquad (23)$$

and

$$\eta_a = A \exp(\Delta E/RT) \quad , \quad T < \text{softening pt.} \qquad (24)$$

It is clear from the figures that within their ranges, A, A', ΔE, and $\Delta E'$ are constants. ΔE and $\Delta E'$ have units of energy and are referred to as the apparent activation energies of the asphalt. Based on the theory of rate processes, Glasstone et al. (11) have shown that the constant A can be related to the molar volume of the material, entropy of activation, and Planek's constant such that:

$$A = \frac{hN}{V} \exp(-\Delta S/R) \qquad (25)$$

where h is Planck's constant, N is Arogadro's number, V is the molar volume of the material in the liquid state, and ΔS is the change in entropy of activation. From figure 15, it can be seen that $A > A'$ and that $\Delta E' > \Delta E$. In other words, around the point of curvature, either the entropy of activation or the molar volume, or both must decrease with an increase in test temperature.

For that straight line portion of the viscosity-temperature curve that lies at temperatures below

the point of curvature (the upper straight line portion), when equation (25) is substituted into equation (24), it results in:

$$\eta_a = \frac{hN}{V} \exp(-\Delta S/R) \exp(\Delta E/RT) \qquad (26)$$

Defining the free energy of activation as:

$$\Delta F = \Delta E - T\Delta S \qquad (27)$$

gives:

$$\eta_a = \frac{hN}{V} \exp(\Delta F/RT) \qquad (28)$$

Glasstone et al. (11) have suggested, and Herrin and Jones (2) have shown for asphalt, that over a normal range of temperatures below the softening point, the entropy of the system can be taken as a constant. Therefore, since ΔS is the change in entropy:

$$A = \frac{hN}{V} \exp(\Delta S/R) = \frac{hN}{V} \qquad (29)$$

and $\Delta F = \Delta E$. Then the apparent energy of activation, ΔE , or the free energy of activation, ΔF , can be calculated from the slope of the lines in figure 15.

Assuming that similar assumptions about the behavior of the entropy of activation can be made at temperatures within the range of this study, and above the point of curvature, the activation energy, $\Delta E'$, may also be calculated. The curves in figure 15 show that ΔE, and therefore, ΔF , are constant

for the range of temperature also.

Another approach to thermodynamic analysis is based on the shift factor as calculated from the principle of reduced variables. From equation (13), it is apparent that:

$$\ln [a_T (T/T_o)] = \Delta E/R \, (1/T - 1/T_o) \qquad (30)$$

It can be seen that the slopes of the curves in Figure 19 are $\Delta E/2.303R$, and therefore, the apparent activation energy may be calculated from the shift factor-temperature relationship. As shown in this figure, the apparent activation energy is constant for the range of temperatures below approximately the softening points of the asphalts. A second range of constant is shown for temperatures above the softening points. The figure also demonstrates the differences in flow behavior among the three asphalts. For the lower temperature range, the B-3056 asphalt was shown to be the most non-Newtonian, and it has the highest activation energy as demonstrated by the steepness of the curve in this temperature range. Above the softening point, all three asphalts display Newtonian behavior and have apparent activation energies that are of the same order of magnitude.

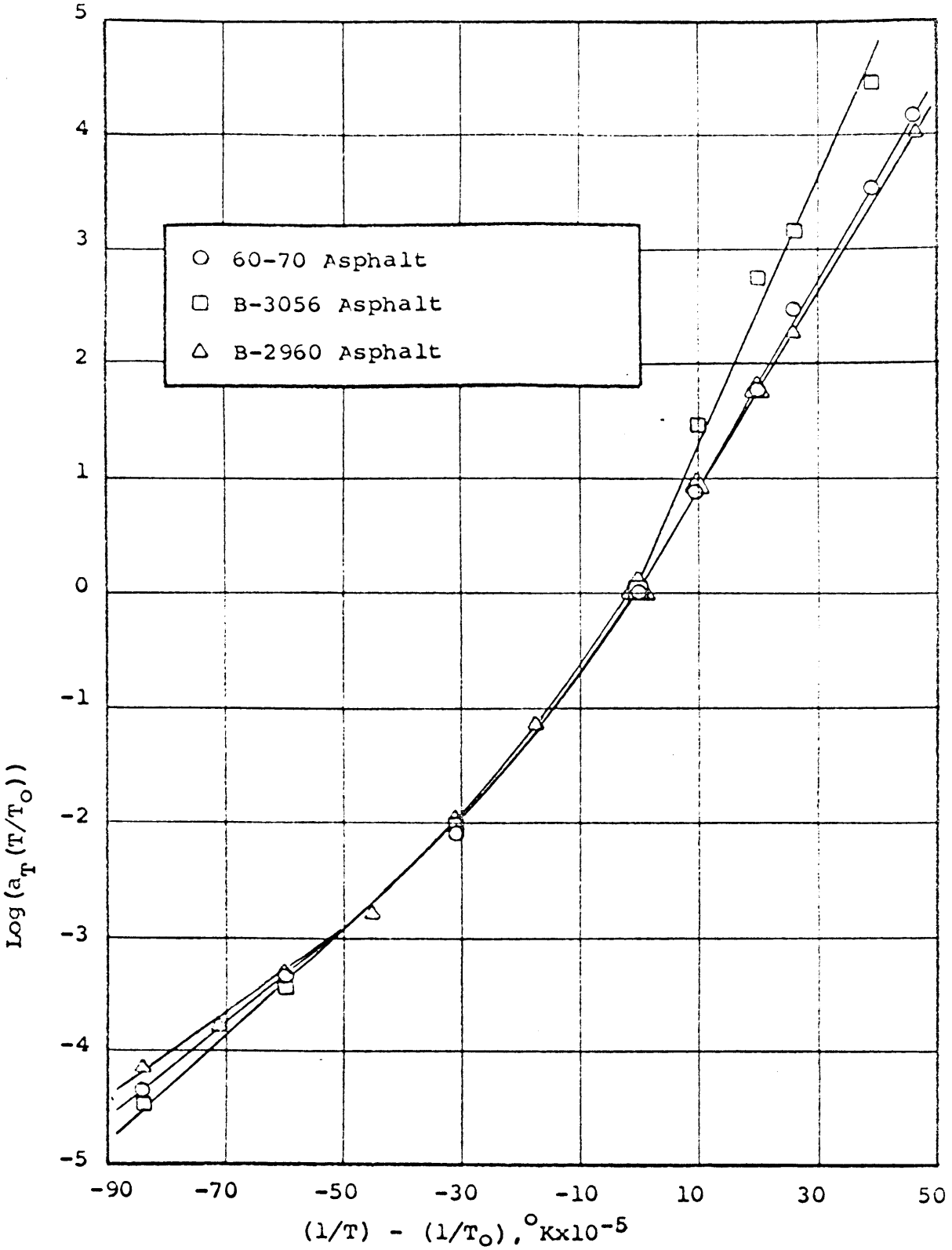

Figure 19 - Log ($a_T(T/T_o)$) versus $(1/T)-(1/T_o)$ for all Asphalts at $T_o=318^oK$.

A third approach to thermodynamic analysis is derived from the theory of rate processes. The hyperbolic sine relationship, as shown by equation (5), has two parameters which, for the three asphalts in this investigation, were evaluated using a computerized curve fitting process. The logrithmic form of equation (6) is:

$$\log(A/T) = \log(K/h) + \Delta S/2.303R - \Delta E/2.303R\,(1/T) \qquad (31)$$

where $A \equiv \eta_o$. But since the first two terms on the right side of the equation may be considered constant, the slope of the semi-log plot A/T versus $1/T$ is $\Delta E/2.303R$. Figure 20 is such a plot for the three asphalts used in this study. The drawing of curves on this figure was very subjective due to the wide scatter of the data points. The particular curve forms were taken from previous analysis and applied to the available data points as best as possible. The curves, therefore, show the characteristics of the other curves previously determined in the thermodynamic analysis.

Table 2 is a tabulation of the apparent activation energies as calculated by the three methods of analysis for each of the three asphalts in both the high and low temperature ranges. The values calculated from the viscosity-temperature and the shift factor-temperature

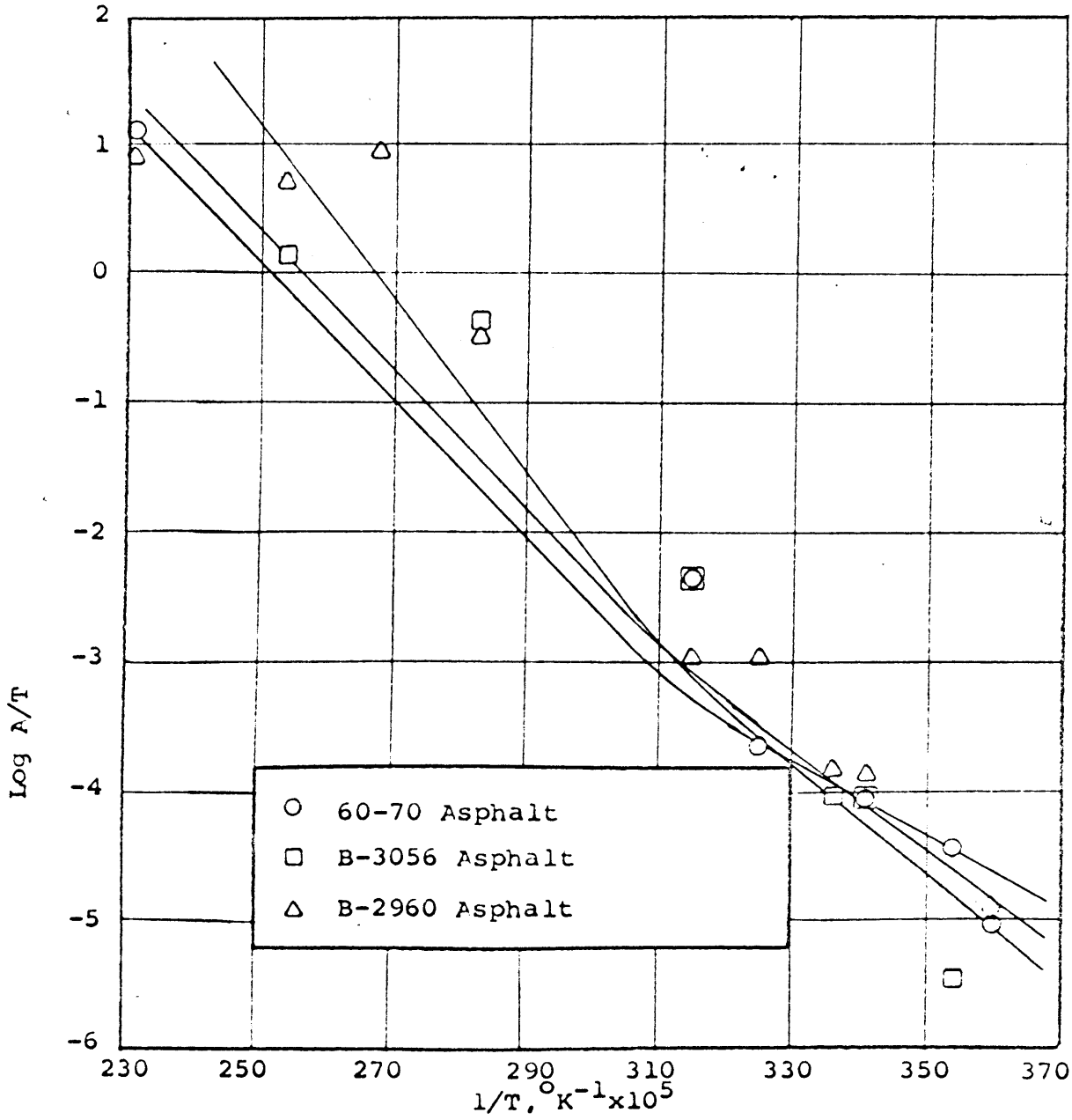

Figure 20 - Log A/T versus 1/T for the three Asphalts

Table 2 - A Comparison of Apparent Activation as Calculated by Different Methods

Asphalt	Temperature Range	E Kcal/^{o}K mole Calculated From		
		Figure 15	Figure 19	Figure 20
60/70 Pene.	high	20.8	19.1	13.5
	low	45.0	41.0	24.1
B-3056	high	20.8	21.8	19.5
	low	53.9	53.9	29.9
B-2960	high	18.35	16.95	17.6
	low	39.3	39.3	24.5

relationships compare very well. The deviation of the values calculated from the hyperbolic sine relationship may be due to the process by which they were calculated in that two curve fitting approximations were used; first in fitting the original flow curve to the data points, and second in finding the hyperbolic sine parameters. In the second case, the parameters were relatively insensitive to small changes in the original data points, but were highly sensitive to changes in each other. Another suggestion for the observed variation is presented in the discussion of the hyperbolic sine relationship.

Concentrating on the value of apparent activation energy as calculated by the first two methods, the values for all three asphalts at high temperatures are less than half the values at low temperatures. Both the 60-70 penetration grade and the B-2960 asphalts have a ratio of high temperature $\Delta E's$ to low temperature $\Delta E's$ of 0.46 ± 0.01. These two asphalts have previously shown similar behavior. The B-3056 has a ratio of 0.40 ± 0.01, and has previously shown consistantly different behavior than the other two asphalts. It is possible then, that this ratio could be used as an index of flow behavior over a wide range of temperature.

Hyperbolic Sine Model

A predominate analysis of the structural flow behavior of asphalt is the hyperbolic sine model as developed from the theory of rate processes. The model has two parameters, A and B, such that:

$$\gamma^{\circ} = A \sinh(B\tau) \qquad (32)$$

A computer program was developed to fit the two parameters to the experimental data. The program provides by trial and error the best fit A and B for each set of data in a least square sense. These A's and B's and the computer program are presented in Appendix II.

According to the present development of the analysis, the parameter A can be related, through temperature, to thermodynamic concepts of the flow behavior as shown in the previous section. The parameter B can be related to the size or volume of the fundamental flow unit. As previously derived from the theory of rate processes, equation (7), the flow unit size is 2KBT where K is Boltzman's constant, and T is the absolute test temperature. Accordingly, the flow unit size, V_f, was calculated and plotted against temperature in figure 21 for the three asphalts. Previous investigation (2) of the change of flow unit size with temperature has indicated that the

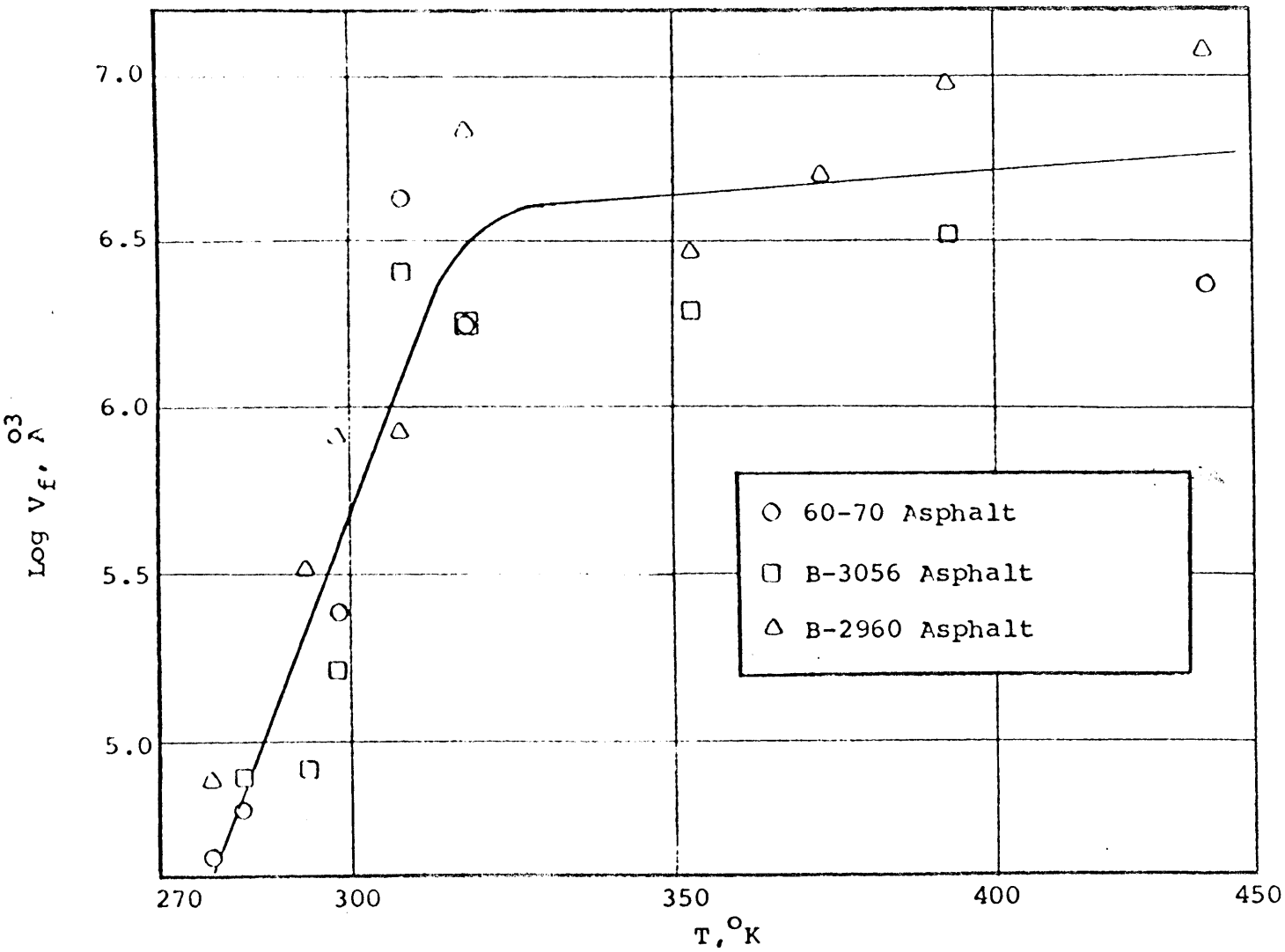

Figure 21 - Flow Unit Size versus Absolute Test Temperature for All Asphalts.

flow unit size markedly decreases with an increase in temperature, and especially in the lower temperature region. Figure 21 shows contrary behavior. Although the results are seemingly inconsistent, two points can be observed which would tend to validate the data. First, the order of magnitude of flow unit size is comparable to the results of other studies. Second, the break in the curve is in the same region of temperature as the similar transitions discussed earlier. Then, either the determination of B is dependent on the curve fitting process used, or there are limitations on the application of the hyperbolic sine relationship that have been exceeded in the testing program.

As mentioned before, the computer program developed to evaluate the parameters A and B of equation (32) was a trial and error procedure based on a least squares best fit. Briefly, a value of 10^{-9} was assumed for B, the value of A was calculated for each data point (τ, $\dot{\gamma}$), and the least squares variation of A was reported as an error term. B was incremented in equal log steps to a value of 10^{0}, and the values of A and B giving a minimum error term were reported in Appendix II. In almost all cases the error term slowly decreased to a minimum value, then increased sharply as B increased. Up to the minimum

error term, the values of A were rather insensitive to changes in B, but the sensitivity increased sharply with the increase in the error term. Because of this sensitivity, and because the computer evaluation of the hyperbolic sine term used a truncated series, there is a possibility that the values of A and B are dependent on this particular evaluation procedure.

In order to examine the other possibility for the conflicting values, a further examination of the hyperbolic sine relationship seemed appropriate. Eyrings flow relation can be written as:

$$\eta = \frac{\tau\delta_1}{2\dot{\gamma}}\left(\frac{h}{KT}\right)\exp\left(\frac{\Delta E - T\Delta S}{RT}\right)\operatorname{csch}\left(\frac{\tau\dot{\gamma}\delta_2\delta_3}{2KT}\right) \qquad (33)$$

Bestul and Belcher (20) have shown that differentiating this equation with respect to $1/T$, once at constant shear stress and once at constant shear rate, gives:

$$\frac{\Delta F_\tau}{R} \equiv \left[\frac{\partial \ln \eta}{\partial(1/T)}\right]_\tau = \frac{\Delta E}{R} + T - (\tau\delta\delta_2\delta_3/2K)\coth\left(\frac{\tau\dot{\gamma}\delta_2\delta_3}{2KT}\right) \qquad (34)$$

and

$$\frac{\Delta F_{\dot{\gamma}}}{R} \equiv \left[\frac{\partial \ln \eta}{\partial(1/T)}\right]_{\dot{\gamma}} = -T + \left(\frac{\Delta E}{RT} + 1\right)\left(\frac{2KT^2}{\tau\dot{\gamma}\delta_2\delta_3}\right)\tanh\left(\frac{\tau\dot{\gamma}\delta_2\delta_3}{2KT}\right) \qquad (35)$$

In other words, a change in viscosity with a change in temperature is dependent on the shear stress or shear rate at which it is measured. Further, the nature of the equations show that the change in viscosity decreases and

eventually becomes negative. Since for asphaltic materials, the change in viscosity with reciprocal of temperature is always positive, there exists some shear stress above which the hyperbolic sine relationship cannot represent the flow behavior of the material.

In order to obtain an approximate value for this critical shear stress, equation (34) may be written as:

$$\frac{\Delta F_\tau}{R} = \frac{\Delta E}{R} + T - \tau B T \coth(\tau B) \qquad (36)$$

The value of $\Delta E/R$ may be calculated as the slope of the curves in figure 20, and B may be calculated from figure 21 or read from the table in Appendix II. The values used for the three asphalts are given in table 3.

By substituting these values into equation (36) and varying the shear stress, the curves in figure 22 could be plotted. This figure shows that the change of viscosity with the reciprocal of absolute temperature is zero at a shear stress of approximately 10^6 dynes/cm^2 according to the hyperbolic sine relationship. Furthermore, this change begins to decrease from a constant value for these three asphalts at a shear stress of about 10^4 dynes/cm^2. Referring to the tables in Appendix I it is observed that a good portion of the viscosity data obtained in this study was taken at shear stresses above 10^4 dynes/cm^2.

Table 3 - Values for Critical Stress Calculation Taken at 300°K.

Asphalt Type	Temperature °K	E Kcal/mole °K	B
60-70	300	21.4	0.50×10^{-4}
B-3056	300	32.0	0.20×10^{-4}
B-2960	300	24.6	0.10×10^{-4}

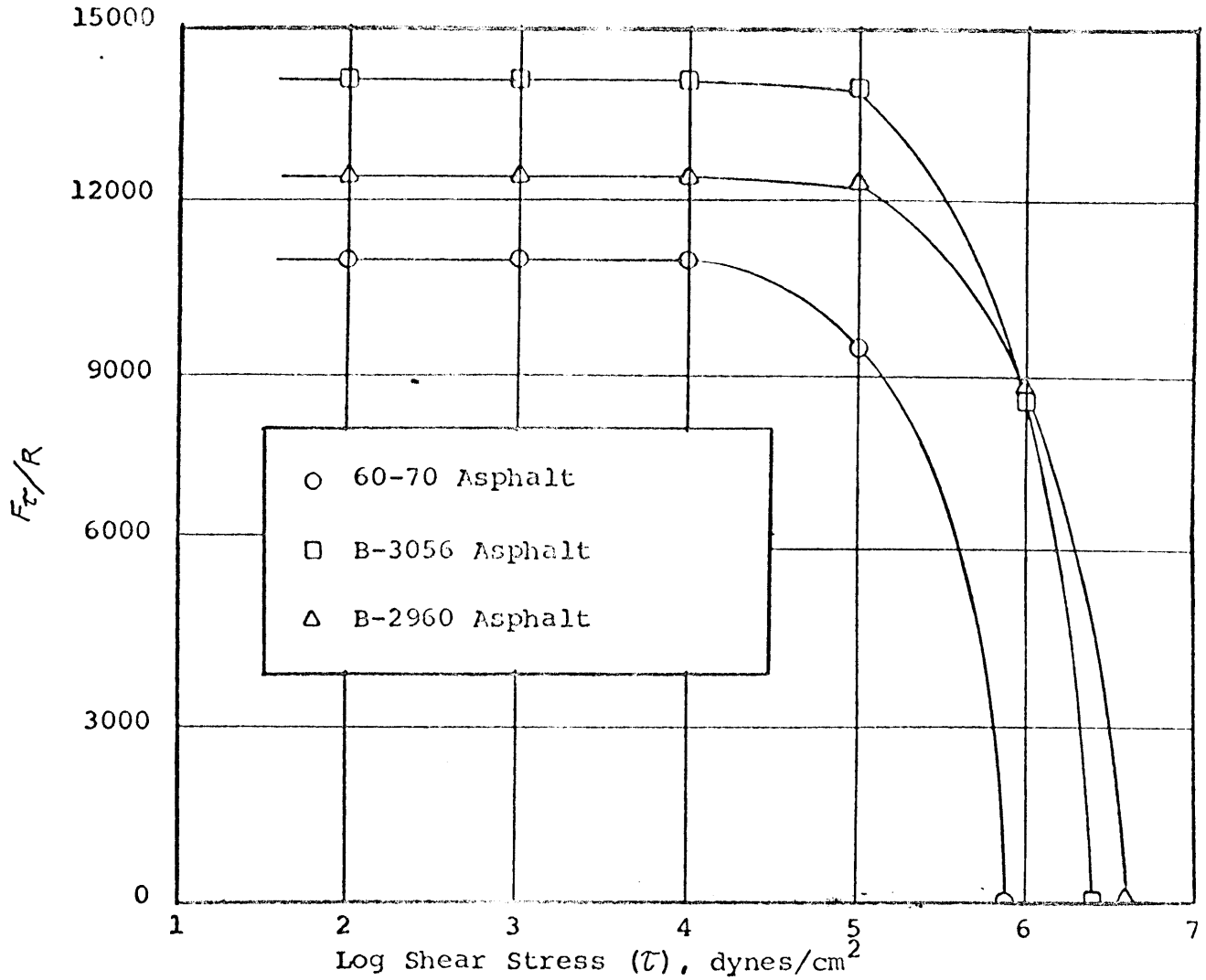

Figure 22 - Change of Viscosity with Inverse Absolute Temperature versus Shear Stress for All Asphalts Using the Hyperbolic Sine Model.

This would indicate that for the data obtained, the hyperbolic sine model could not be used to represent the flow behavior of the material. It is suggested that for this reason, the calculated values of thermodynamic constants from the A/T versus $1/T$ curves do not compare with values calculated by other means, and, the values calculated for the flow unit size contradict the trends observed in previous works.

The hyperbolic sine model has been shown to be a successful means to predict the flow behavior of asphalt. It has also been used to advantage in the calculation of certain thermodynamic constants and flow unit sizes. It has the characteristics of a very useful tool in the understanding of the flow mechanism. The investigator, however, must be constantly aware of the limitations of the model and confine the variation of the test parameters to conform with these limitations.

SUMMARY AND CONCLUSIONS

This study briefly reviews some concepts suggested to analyze the flow characteristics of rheological materials with emphasis on those which are promising in the analysis of flow of asphalts. The suggested concepts are catagorized as experimental, mathematical, structural, physical-chemical, and thermal. It is shown that for the three asphalts used, it is possible to construct flow diagrams over a wide range of shear stress, shear rate, and temperature using different viscometers and the principle of reduced variables. Thermodynamic analysis is used to study thermal characteristics of flow behavior. An application of Eyring's rate process theory to the analysis of asphalt flow is examined and the variation of viscosity, determined at constant shear stress or constant shear rate, with temperature is discussed. From this study, the following conclusions are drawn:

1. The flow data, when obtained by different viscometers, are consistent. Therefore, different viscometers can be used to obtain shear data over a wide range of shear rate or shear stress.

2. Logrithmic plots of viscosity, shear stress, and shear rate produce, in general for these three asphalts,

straight lines. Therefore, a power function may be used as a first approximation to represent the flow behavior.

3. The temperature dependency of viscosity requires that viscosity variation with temperature at fixed shear stress be larger than that at fixed shear rate.

4. For the three asphalts used in this study, the viscosity-temperature relationship is continuous and a sharp transition occurs at about the ring and ball softening point

5. The principle of reduced variables may be used to further extend the range of the shear rate data by reducing the data obtained at different temperatures to an arbitrary base temperature.

6. Thermodynamic parameters may prove to be of great value in the analysis of asphalt flow. The ratio of the apparent energy of activation at high temperatures (above the softening point) to low temperatures (below the softening point) was for these three asphalts, an indication of their deviation from Newtonian flow behavior.

7. An examination of the applicability of Eyring's hyperbolic sine relation to the analysis

of the flow of these three asphalts revealed that; a) for these three materials there exists critical shear stresses, beyond which the hyperbolic sine relation fails to represent the flow behavior of each material, and b) when these critical shear stresses are within the experimental range, the flow results cannot be represented by such a relationship.

SUGGESTIONS FOR FUTURE WORK

Future work in the rheology of asphalt should include the following areas:

1. Attempts should be made to broaden the ranges of measurable flowparameters with instruments such as rheogonometers which are capable of wide range operation. Special interest should be taken in the extreme low temperature ranges at low shear rates.

2. These studies should be broadened to incorporate more asphalts of different origins and types to check the validity of the general application of the presently known analytical techniques.

3. More thorough studies of thermo-dynamic analysis should be made with the objective of more precise analysis. Eyring's hyperbolic sine relationship should be investigated to precisely determine the extent of its usefulness.

LIST OF REFERENCES

1. Schweyer, H.E., "Asphalt Composition and Properties," Highway Research Board, Bulletin 192, 1958.

2. Herrin, M. and Jones, G.E., "The Behavior of Bituminous Materials from the Viewpoint of the Absolute Rate Theory," Proceedings, Association of Asphalt Paving Technologists, Volume 32, 1963.

3. Majidzadeh, K. and Schweyer, H.E., "Non-Newtonian Behavior of Asphalt Cements," A paper presented to the Annual Meeting of the Association of Asphalt Paving Technologists, February, 1965.

4. Traxler, R.N., "Rheology and Rheological Modifers other than Elastomers: Structure and Time," Bituminous Materials; Asphalts, Tars, and Pitches, A.J. Hoiberg, ed., Interscience Publishers, New York, 1964.

5. Andrade, E.N. da C., Viscosity and Plasticity, Chemical Publishing Co., Inc., New York, 1951.

6. Maxwell, C., "Dynamical Theory of Cases," Scientific Papers, Volume 2, pg. 31.

7. Mooney, M. "A Theory of the Viscosity of a Maxwellian Elastic Liquid," Transactions of the Society of Rheology, Volume 1, 1957.

8. Denny, D.A. and Brodkey, R.S., "Kinetic Interpretation of Non-Newtonian Flow," Journal, Applied Physics, Volume 33, No. 7, pg. 2269, 1962.

9. Denny, D.A., Kim, H.T., and Brodkey, R.S., "Kinetic Interpretation of Non-Newtonian Flow," A paper presented at the annual meeting of the Society of Rheology, October, 1964.

10. Brodkey, Robert S., unpublished notes.

11. Glasstone, S., Laidler, K., and Eyring, H., The Theory of Rate Processes, McGraw-Hill Book Company, Inc., New York, 1941.

12. Nellensteyn, F.J., Journal, Institute of Petroleum Technology, 1924.

13. Mack, C., "Physical Chemistry," Bituminous Materials: Asphalts, Tars, and Pitches, A.J. Hoiberg, ed., Interscience Publishers, New York, 1964.

14. Katz, D.L. and Beu, K.E., Industrial and Engineering Chemistry, 1945.

15. Swanson, J.M., Journal of Physical Chemistry, 1942.

16. Neppe, S.L., "Classification of Bitumens in Asphalt Technology by Certain Rheological Properties," Journal of the Institute of Petroleum, Part I, pg. 38, 1952.

17. Ferry, J.D., Viscoelastic Properties of Polymers, John Wiley and Sons, Inc., New York, 1961.

18. Van Wazer, J.R., Lyons, J.W., Kim, K.Y., and Colwell, R.E., Viscosity and Flow Measurement, Interscience Publishers, New York, 1963.

19. Brodkey, R.S., "Translating Terms for Non-Newtonian Flow," Industrial and Engineering Chemistry, Volume 54, September, 1962.

20. Bestul, A.B. and Belcher, H.V., "Temperature Coefficients of Non-Newtonian Viscosity at Fixed Rate of Shear," Journal of Applied Physics, Volume 24, No. 6, June, 1953.

21. Traxler, R.N. and Schweyer, H.E., Physics, 7,67,1936.

APPENDIX I

RHEOLOGIC DATA

Description	Shear Stress dynes/cm^2	Shear Rate sec^{-1}	Viscosity poises
Asphalt Type 60/70 Penetration			
-10°C	2.39×10^7	1.70×10^{-3}	1.41×10^{10}
- 5°C	1.06×10^7	1.70×10^{-3}	6.24×10^9
	1.49×10^7	4.30×10^{-3}	3.47×10^9
	1.79×10^7	8.48×10^{-3}	2.11×10^9
0°C	5.19×10^6	1.70×10^{-3}	3.05×10^9
	8.25×10^6	6.40×10^{-3}	1.29×10^9
	1.23×10^7	1.83×10^{-2}	6.72×10^8
	1.74×10^7	4.40×10^{-2}	3.95×10^8
5°C	3.30×10^5	6.70×10^{-4}	4.93×10^8
	7.00×10^5	1.11×10^{-3}	6.31×10^8
	1.65×10^6	3.08×10^{-3}	5.36×10^8
	4.50×10^6	1.15×10^{-2}	3.91×10^8
	1.00×10^7	5.20×10^{-2}	1.92×10^8
10°C	1.61×10^5	1.42×10^{-3}	1.13×10^8
	3.50×10^5	2.67×10^{-3}	1.31×10^8
	6.00×10^5	4.68×10^{-3}	1.28×10^8
	1.20×10^6	1.12×10^{-2}	1.07×10^8
	1.65×10^6	1.73×10^{-2}	9.54×10^7
20°C	1.60×10^4	1.31×10^{-3}	1.22×10^7
	3.00×10^4	2.56×10^{-3}	1.17×10^7
	5.50×10^4	4.90×10^{-3}	1.12×10^7
	3.55×10^5	3.62×10^{-2}	9.81×10^6
25°C	2.50×10^3	8.75×10^{-4}	2.86×10^6
	6.00×10^3	2.29×10^{-3}	2.62×10^6
	1.20×10^4	4.59×10^{-3}	2.62×10^6
	3.50×10^4	1.43×10^{-2}	2.45×10^6
	8.10×10^5	3.43×10^{-2}	2.36×10^6
35°C	8.10×10^2	2.37×10^{-3}	3.42×10^5
	1.50×10^3	4.70×10^{-3}	3.19×10^5

Description	Shear Stress dynes/cm^2	Shear Rate sec^{-1}	Viscosity poises
Asphalt Type 60/70 Penetration			
35°C	4.00×10^3	1.39×10^{-2}	2.88×10^5
	9.00×10^3	3.40×10^{-2}	2.65×10^5
	1.63×10^4	6.55×10^{-2}	2.49×10^5
45°C	2.80×10^2	6.48×10^{-3}	4.32×10^4
	9.00×10^2	2.21×10^{-2}	4.07×10^4
	2.80×10^3	7.45×10^{-2}	3.76×10^4
	9.50×10^3	2.67×10^{-1}	3.56×10^4
	3.00×10^4	9.10×10^{-1}	3.30×10^4
80°C	2.38×10^2	7.40×10^{-1}	3.22×10^2
	7.00×10^2	2.17×10^0	3.23×10^2
	1.80×10^3	5.55×10^0	3.24×10^2
	5.50×10^3	1.68×10^1	3.27×10^2
	1.78×10^4	5.43×10^1	3.28×10^2
120°C	4.10×10^2	2.68×10^1	1.53×10^1
	9.00×10^2	5.88×10^1	1.53×10^1
	1.80×10^3	1.19×10^2	1.51×10^1
	4.00×10^3	2.60×10^2	1.53×10^1
	7.70×10^3	5.00×10^2	1.54×10^1
160°C	8.15×10^2	5.22×10^2	1.56×10^0
	1.40×10^3	8.95×10^2	1.56×10^0
	2.80×10^3	1.79×10^3	1.56×10^0
	4.00×10^3	2.56×10^3	1.56×10^0
	5.00×10^3	3.20×10^3	1.56×10^0
Asphalt Type B-3056			
10°C	4.00×10^5	2.70×10^{-4}	1.48×10^9
	6.50×10^5	5.15×10^{-4}	1.26×10^9
	9.50×10^5	1.02×10^{-3}	9.31×10^8
	1.30×10^6	1.77×10^{-3}	7.34×10^8
	1.64×10^6	2.68×10^{-3}	6.12×10^8

Description	Shear Stress dynes/cm	Shear Rate sec^{-1}	Viscosity poises
Asphalt Type B-3056			
20°C	1.15×10^{5}	1.84×10^{-3}	6.25×10^{7}
	2.20×10^{5}	4.40×10^{-3}	5.00×10^{7}
	3.80×10^{5}	9.35×10^{-3}	4.06×10^{7}
	7.00×10^{5}	2.07×10^{-2}	3.38×10^{7}
	1.16×10^{6}	4.08×10^{-2}	2.84×10^{7}
25°C	4.80×10^{4}	2.08×10^{-3}	2.31×10^{7}
	8.00×10^{4}	3.81×10^{-3}	2.10×10^{7}
	1.50×10^{5}	8.15×10^{-3}	1.84×10^{7}
	2.70×10^{5}	1.62×10^{-2}	1.66×10^{7}
	4.90×10^{5}	3.35×10^{-2}	1.46×10^{7}
35°C	3.28×10^{3}	2.40×10^{-3}	1.37×10^{6}
	6.00×10^{3}	4.77×10^{-3}	1.26×10^{6}
	1.00×10^{4}	8.53×10^{-3}	1.17×10^{6}
	1.80×10^{4}	1.66×10^{-2}	1.08×10^{6}
	3.20×10^{4}	3.15×10^{-2}	1.02×10^{6}
45°C	7.10×10^{2}	1.83×10^{-2}	3.88×10^{4}
	2.00×10^{3}	4.01×10^{-2}	4.99×10^{4}
	5.00×10^{3}	1.39×10^{-1}	3.60×10^{4}
	1.50×10^{4}	4.38×10^{-1}	3.42×10^{4}
	2.90×10^{4}	8.65×10^{-1}	3.35×10^{4}
80°C	2.68×10^{2}	8.80×10^{-1}	3.05×10^{2}
	7.00×10^{2}	2.38×10^{0}	2.94×10^{2}
	1.80×10^{3}	5.90×10^{0}	3.05×10^{2}
	3.20×10^{3}	1.03×10^{1}	3.11×10^{2}
	7.50×10^{3}	2.44×10^{1}	3.07×10^{2}
120°	2.28×10^{2}	1.87×10^{1}	1.22×10^{1}
	5.00×10^{2}	4.10×10^{1}	1.22×10^{1}
	1.20×10^{3}	9.95×10^{1}	1.21×10^{1}
	2.50×10^{3}	2.04×10^{2}	1.23×10^{1}

Description	Shear Stress dynes/cm^2	Shear Rate sec $^{-1}$	Viscosity poises
Asphalt Type B-3056			
120°C	6.50×10^3	5.35×10^2	1.21×10^1
140°C	2.16×10^2	6.65×10^3	3.25×10^0
	3.40×10^3	1.03×10^3	3.30×10^0
160°C	1.18×10^3	9.25×10^2	1.28×10^0
	2.00×10^3	1.60×10^3	1.25×10^0
	2.93×10^3	2.32×10^3	1.26×10^0
Asphalt Type B-2960			
5°C	4.56×10^5	1.20×10^{-3}	3.80×10^8
	9.00×10^5	3.40×10^{-3}	2.64×10^8
	1.40×10^6	7.00×10^{-3}	2.00×10^8
	1.75×10^6	9.50×10^{-3}	1.84×10^8
10°C	1.80×10^5	1.40×10^{-3}	1.28×10^8
	4.80×10^5	6.00×10^{-3}	8.00×10^7
	8.15×10^5	1.30×10^{-2}	6.27×10^7
	1.40×10^6	3.00×10^{-2}	4.66×10^7
20°C	1.55×10^4	2.50×10^{-3}	6.20×10^6
	3.58×10^4	6.00×10^{-3}	5.96×10^6
	8.60×10^4	1.50×10^{-2}	5.73×10^6
	1.66×10^4	3.00×10^{-2}	5.55×10^6
25°C	7.80×10^3	2.80×10^{-3}	2.78×10^6
	1.52×10^4	6.00×10^{-3}	2.53×10^6
	3.46×10^4	1.50×10^{-2}	2.30×10^6
	8.20×10^4	4.20×10^{-2}	1.95×10^6
35°C	1.50×10^3	4.00×10^{-3}	3.75×10^5
	3.56×10^3	1.00×10^{-2}	3.56×10^5
	9.65×10^3	3.00×10^{-2}	3.22×10^5
	3.20×10^4	1.10×10^{-1}	2.91×10^5
45°C	7.80×10^2	1.60×10^{-2}	4.87×10^4
	1.70×10^3	4.00×10^{-2}	4.25×10^4

Description	Shear Stress dynes/cm^2	Shear Rate sec^{-1}	Viscosity poises
Asphalt Type B-2960			
45°C	3.40×10^3	9.50×10^{-2}	3.58×10^4
	7.85×10^3	2.50×10^{-1}	3.14×10^4
	1.60×10^4	6.00×10^{-1}	2.66×10^4
60°C	5.50×10^3	2.50×10^0	2.20×10^3
	7.86×10^3	3.68×10^0	2.19×10^3
	1.32×10^4	6.00×10^0	2.20×10^3
	1.87×10^4	8.50×10^0	2.20×10^3
80°C	3.10×10^2	9.00×10^{-1}	3.44×10^2
	1.10×10^3	3.20×10^0	3.44×10^2
	2.86×10^3	8.50×10^0	3.36×10^2
	8.50×10^3	2.50×10^1	3.40×10^2
	1.65×10^4	5.00×10^1	3.30×10^2
100°C	3.40×10^3	7.50×10^1	4.53×10^1
	5.40×10^3	1.20×10^2	4.50×10^1
	8.00×10^3	1.80×10^2	4.44×10^1
120°C	3.10×10^2	1.80×10^1	1.72×10^1
	9.50×10^2	6.00×10^1	1.58×10^1
	2.90×10^3	2.00×10^2	1.45×10^1
	4.45×10^3	3.20×10^2	1.45×10^1
	8.00×10^3	6.00×10^2	1.33×10^1
140°C	3.22×10^3	8.00×10^2	4.02×10^0
	3.82×10^3	9.50×10^2	4.02×10^0
	4.84×10^3	1.20×10^3	4.03×10^0
160°C	1.45×10^3	8.00×10^2	1.81×10^0
	1.75×10^3	9.50×10^2	1.84×10^0
	2.90×10^3	1.60×10^3	1.81×10^0
	4.45×10^3	2.50×10^3	1.78×10^0

APPENDIX II

HYPERBOLIC SINE MODEL

PARAMETERS

AND

COMPUTER PROGRAM

Description	Temperature, °C	A	B
60-70	5	2.63×10^{-3}	6×10^{-7}
	10	9.95×10^{-3}	8×10^{-7}
	20	2.84×10^{-2}	3×10^{-6}
	35	7.21×10^{-2}	5×10^{-5}
	45	1.43×10^{0}	2×10^{-5}
	160	3.20×10^{4}	2×10^{-5}
B-3056	10	1.03×10^{-3}	1×10^{-6}
	20	2.77×10^{-2}	1×10^{-6}
	25	2.89×10^{-2}	2×10^{-6}
	35	2.84×10^{-2}	3×10^{-5}
	45	1.41×10^{0}	2×10^{-5}
	80	1.62×10^{2}	2×10^{-5}
	120	2.73×10^{3}	3×10^{-5}
B-2960	5	3.47×10^{-3}	1×10^{-6}
	20	4.21×10^{-2}	4×10^{-6}
	25	4.53×10^{-2}	1×10^{-5}
	35	3.35×10^{-1}	1×10^{-5}
	45	3.62×10^{-1}	8×10^{-5}
	80	9.70×10^{1}	3×10^{-5}
	100	4.39×10^{2}	5×10^{-5}
	120	7.67×10^{2}	9×10^{-5}
	160	5.44×10^{3}	1×10^{-4}

Fortran Program for the Calculation of A and B
in the Hyperbolic Sine Model

```
      DIMENSION GAMMA(50),TAU(50),SINCH(50)
      DO 8 KKK=1,1000
      READ 154
  154 FORMAT(72H
     1                  )
      PRINT 154
      READ 3,N,(TAU(I),GAMMA(I),I=1,N)
    3 FORMAT(15/(2E15.8))
      PRINT 155,N,(GAMMA(I),TAU(I),I=1,N)
  155 FORMAT (5HN IS 13/22HGAMMA DOT         TAU/(2E11.4))
      PRINT 156
  156 FORMAT (7X1HA14X1HB8X5HERROR)
      DO 20 K=1,7
      KL=10-K
      E=1./(10.**KL)
      DO 20 KK=1,10
      AB=KK
      B=AB*E
    1 SUM=0.
      SUMD=0.
      AMIN1=0.
      DO 4 I=1,N
      C=B*TAU(I)
      SINCH(I)=C+C**3/6.+C**5/120.
      SUM=SUM+GAMMA(I)*SINCH(I)
    4 SUMD=SUMD+(SINCH(I))**2
      A=SUM/SUMD
      DO 5 I=1,N
    5 AMIN1=AMIN1+(GAMMA(I)-A*SINCH(I))**2
   20 PRINT 71, A, B, AMIN1
   71 FORMAT(3E15.8)
    8 CONTINUE
      CALL EXIT
      END
```